JOURNAL OF RESEARCH of the National Bureau of Standards—D. Radio Propagation
Vol. 66D, No. 6, November–December 1962

Propagation of Terrestrial Radio Waves of Long Wavelength—Theory of Zonal Harmonics With Improved Summation Techniques[1]

J. R. Johler and L. A. Berry

Contribution From Central Radio Propagation Laboratory, National Bureau of Standards, Boulder, Colo.

(Received January 18, 1962; revised June 15, 1962)

The rigorous mathematical treatment for the propagation of a radio wave from a Hertz-dipole-source current-moment around a finitely conducting spherical earth surrounded by a concentric electron-ion plasma can be expressed as a series of zonal harmonics. Such a solution to the problem was obtained for the terrestrial sphere without a concentric plasma many years ago (1904–1915). However, the summation of the series, even at long wavelengths or low frequencies, was considered to be impractical and the well-known and, indeed, rigorous Watson transformation was introduced (1918).

The Watson transformation led to the development of elegant mathematical techniques both rigorous and approximate for the evaluation of the fields of radio waves in the vicinity of the earth. However, it does not necessarily follow that the Watson transformation is the only way to achieve numerical mastery of the problem. Indeed, it also does not follow that the Watson transformation is the most efficient approach to the rigorous form of the theory of propagation, especially at long wavelengths.

This paper demonstrates that the field of the propagated long wavelength radio wave (frequencies less than approximately 50 kc/s) can indeed be evaluated by a summation of a series of zonal harmonics. Whereas the number of terms could become quite large (of the order of 10 k_1a where a is the radius of the sphere and k_1 is the wave number of the medium between the concentric plasma and the earth), the speed with which these terms can be summed on a large-scale computer offsets the complications introduced by the Watson transformation as to the rigorous mathematical solution of the problem.

The detailed structure of the field in the absence of a concentric plasma is characterized by the quite regular behavior of the ground wave as a function of distance. Indeed, the steady decrement of the ground-wave field is modified only near the antipode, where an interference pattern or standing wave as a function of distance is noted because of another wave's traveling around the sphere in the opposite direction.

The introduction of the concentric electron-ion plasma shell traps the waves leaking into space, where reflection from the plasma builds up traveling waves in the direction of increased distance from the transmitter. Thus, the series of zonal harmonics comprises individual waves which are traveling in the radial direction with respect to the center of the sphere and standing in the direction of increased angular distance around the sphere. These waves, when summed, build up the wave progressing in the direction of increased angular distance. Under special circumstances, standing waves can be noted. This is especially obvious near the antipode of the transmitter.

The results of the computations indicate that full rigor can be achieved with comparative ease at frequencies less than approximately 50 kc/s, leaving only the assumed model for the transmitter and the propagation medium and avoiding the complications of the Watson transformation.

1. Introduction

The treatment of the propagation of electromagnetic or sound waves diffracted by spherical objects as a series of zonal harmonics was introduced in such early theoretical investigations as those of Lord Rayleigh [1904] and Debye [1909]. The early research work on the radio problem, such as that of Poincaré [1904, 1910], Macdonald [1903, 1904, 1911, 1914], Nicholson [1910, 1911], and Love [1915], attempted to use the theory of zonal harmonics, either by a direct summation or by forming an integral from the series, to explain the "remarkable observed facts

[1] This work was sponsored by the Rome Air Development Center, Griffiss Air Force Base, N.Y., under Tasks 4 and 5 of D.O. No. AF 30(602)-2488. Techniques for summing zonal harmonics and evaluating Bessel functions for ELF/VLF wave propagation were developed for U. S. Navy, ONR, order No. NA-46-59.

648645—62——7

concerning the propagation of radio waves around the earth's curvature." The series, as formulated at this time, was quite difficult to sum because of slow convergence for the radio problem. Love, however, succeeded in summing a large number of terms, but his method was not considered to be completely satisfactory since it involved graphical construction and estimates.

The results of Love, Poincaré, and Nicholson did not explain the propagation around the earth's curvature, since it was correctly concluded for the assumed model that the diffracted field decayed exponentially, $\exp[-\beta (k_1 a)^{\frac{1}{3}}\theta]$, where β is a constant, k_1 is the angular wave number, $k_1 \sim \omega/c$ at a frequency $f=\omega/2\pi$ with c, the speed of light, a is the radius of the spherical earth, and θ is the angular distance measured at the center of the spherical earth, figure 2, from the transmitter.

Since the experimental evidence indicated that the field decayed approximately as $1/\sqrt{d}$ or at most $1/d$, where $d=a\theta$ is the distance along the surface of the earth, March [1912] reformulated the problem as an integral to obtain an answer more consistent with observed facts, and indeed found that the field decayed approximately as $1/\sqrt{\theta \sin \theta} \sim 1/d$ around the earth's curvature. Although the work of March [1912] contained questionable approximations which affected the conclusions, a new approach to the problem had been introduced. March concluded that the waves were propagated without the exponential attenuation and further concluded that the "remarkable propagation of radio waves around the earth was explained." Apparently in answer to a criticism of March's [1912] paper by Poincaré (Poincaré [1904, 1910] previously concluded the wave was damped exponentially with distance), von Rybczynski [1913] extended March's paper and concluded that the exponential factor was neglected by March. He further concluded that this factor would become significant at great distances. However, von Rybczynski concluded that since the experimental results at that time were inconclusive (i.e., the results involved short distances) the significance of the exponential factor had not been established.

In view of the discrepancies in the results of March and others, and apparently at the request of van der Pol, Watson [1918, 1919] reformulated the integrals used by March by means of the well-known Watson transformation and again reached the conclusion that the waves decayed exponentially around the earth's curvature, the experimental evidence notwithstanding. Watson [1919] further postulated a reflector of concentric plasma of high conductivity and reached the conclusion for this theoretical model that the waves did decay approximately as $1/\sqrt{d}$ around the earth's curvature as indicated by the observed facts, not for the reason set forth by March, but as a result of trapping of waves by the ionosphere. The comment of Watson in the 1919 paper "a consequence of its presence (the ionosphere) is that it places grave obstacles in the way of communications with Mars or Venus, if the desirability of communicating with these planets should ever arise" is interesting from today's (1961) perspective.

The Watson transformation seems to be the basis for most theoretical work in subsequent years (1919 to date), and Watson thus becomes the "prophet" of a "new rigor" in the treatment of the propagation of terrestrial radio waves. Thus, for example, the works of van der Pol and Bremmer [1937, 1938, 1949] use the Watson transformation for the radio problem. The treatment of radio wave propagation in the space between the ionosphere and the earth as a waveguide at very low frequencies [Wait, 1957, 1960] has also exploited the Watson transformation. Although the technique of zonal harmonics has been used extensively in the literature on, for example, electromagnetic problems associated with cylinders [Wait, 1959], the application to the terrestrial sphere for the radio problem is confined to the work of Love [1915]. This is probably a consequence of the delusion that the slow convergence of the series of zonal harmonics for the radio-terrestrial sphere problem is an intractable situation.

Whereas the Watson transformation has very great merit from a theoretical point of view and has been exploited extensively in certain theories of propagation, it is appropriate at this

time, especially at the low frequencies or long wavelengths,[2] to re-examine the earlier treatment based on zonal harmonics which was apparently successful in yielding correct conclusions. Indeed, the procedure outlined in this paper, based on recurrence techniques for the calculation of Bessel functions [Goldstein and Thaler, 1959], can, as will be demonstrated herein, yield results quite readily at frequencies less than approximately 50 kc/s. The formulation presented in this paper is completely rigorous and assumes only the models of a Hertzian dipole source current moment and propagation media consisting of a finitely conducting spherical earth with a specified concentric plasma shell. The results can also be extended to stratified spherical earth and indeed to a continuously stratified [Johler and Harper, 1962] concentric plasma, figure 4, as a model ionosphere.

2. Theory of Propagation

The electrodynamic fields $\bar{E}$, volts/meter,[3] and $\bar{H}$ ampere-turns/meter described by Maxwell's equations,

$$\bar{\nabla}\times\bar{E}+\mu_0\frac{\partial}{\partial t}\bar{H}=0$$

$$\bar{\nabla}\times\bar{H}-\epsilon_0\frac{\partial}{\partial t}\bar{E}=\bar{J}\,, \tag{1}$$

where $\bar{J}$ is the conduction or convection current, amperes/square meter, can be treated as a continuous ($t=-\infty$ to $+\infty$) time-harmonic wave, $\bar{E}=\bar{E}(\omega, D)$, $\bar{H}=\bar{H}(\omega, D)$, at a distance, D, from some reference and a frequency, $f=\omega/2\pi$, or,

$$\bar{E}=|\bar{E}|\exp[i\omega t-ikD], \tag{2}$$

where the positive time function is assumed, and the angular-wave number of the medium is represented by $k=\omega\eta/c$, where η is the index of refraction of the medium. Maxwell's equations are therefore wirtten,

$$\mu_0 i\omega\bar{H}+\bar{\nabla}\times\bar{E}=0$$

$$(\epsilon i\omega+\sigma)\bar{E}-\bar{\nabla}\times\bar{H}=0, \tag{3}$$

where ϵ, σ, and μ_0 are the permittivity, farad/meter; the conductivity, mhos/meter; and the permeability, henry/meter, of the medium of propagation respectively.

The spherical coordinate system, figure 1, with the unit vectors, $\bar{r}$, $\bar{\theta}$, $\bar{\phi}$, is introduced for convenience, since the earth and the ionosphere, for example, present approximately spherical boundaries to the propagation media. The origin of the coordinate system is located at the center of the sphere such as illustrated, figure 2. There are six components of the electrodynamic fields in such a coordinate system, E_r, E_θ, E_ϕ, H_r, H_θ, and H_ϕ, which can be calculated by a differentiation process from a single [Hertz, 1889; Debye, 1909] vector, $\bar{\Pi}$, provided the scalar Π satisfies the wave equation in the medium with wave number, k, ($-k^2=\mu_0 i\omega(\epsilon i\omega+\sigma)$)

$$(\nabla^2+k^2)\,\Pi=0, \tag{4}$$

where $\bar{\Pi}=\Pi\bar{a}$ for constant $\bar{a}$, and the operator ∇^2 is defined by eq (55) or,

$$E_r=[\exp(i\omega t)]\left[\frac{-1}{rb\sin\theta}\right]\frac{\partial}{\partial\theta}\left[\sin\theta\,\frac{\partial\Pi^e}{\partial\theta}\right]$$

$$E_\theta=[\exp(i\omega t)]\,\frac{1}{rb}\,\frac{\partial^2}{\partial r\partial\theta}\,[r\Pi^e]$$

[2] Additional general references to the literature of long wavelength radio waves not otherwise cited in this paper but listed under "references" are Campbell [1960]; Jean et al. [1961]; Pierce [1960]; and Wait [1960].

[3] Rationalized mks units are used in this paper.

$$H_\phi = [\exp\ i\omega t)]\,\frac{1}{b}\,\frac{k^2}{\mu_0 i\omega}\,\frac{\partial \Pi^e}{\partial \theta}$$

$$E_\phi = [\exp\ (i\omega t)]\,\frac{\mu_0 i\omega}{b}\,\frac{\partial \Pi^m}{\partial \theta}$$

$$H_r = [\exp\ (i\omega t)]\left[\frac{-1}{rb\,\sin\,\theta}\right]\frac{\partial}{\partial \theta}\left[\sin\,\theta\,\frac{\partial \Pi^m}{\partial \theta}\right]$$

$$H_\theta = [\exp\ (i\omega t)]\,\frac{1}{rb}\,\frac{\partial^2}{\partial r \partial \theta}\,[r\Pi^m] \tag{5}$$

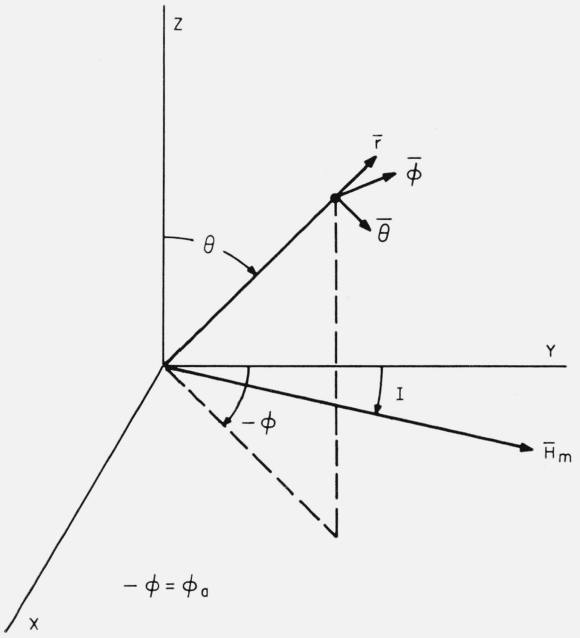

FIGURE 1. *General coordinate systems.*

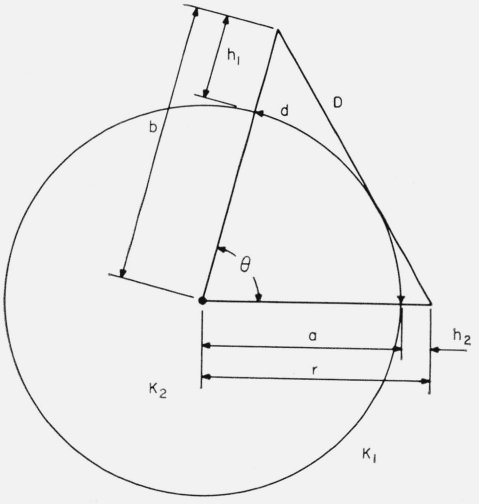

FIGURE 2. *Spherical coordinate systems for model terrestrial sphere of radius,* r=a.

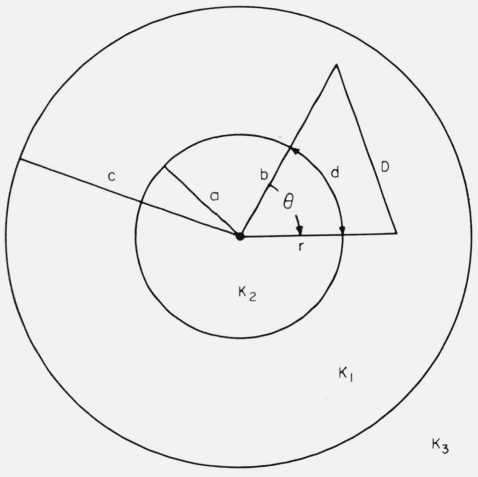

FIGURE 3. *Spherical coordinates for model terrestrial sphere of radius* r=a, *surrounded by concentric plasma from* r=c *to* r=∞.

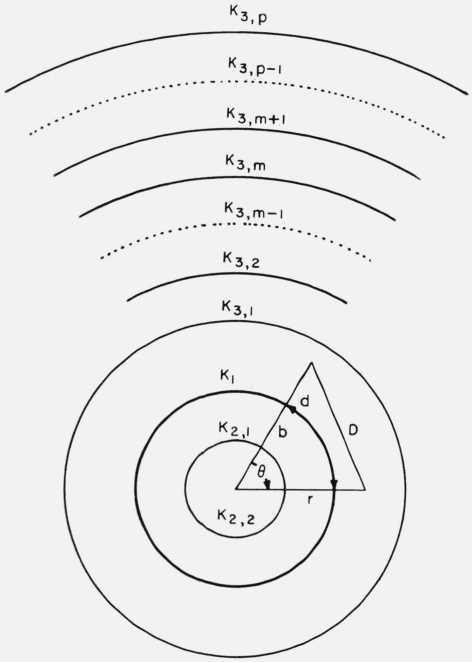

FIGURE 4. *Spherical coordinates, illustrating extension to stratification of terrestrial model sphere and extension to a continuously stratified concentric plasma.*

where Π^m refers to vertical magnetic source dipole or scatter field and Π^e refers to vertical electric source dipole or scatter field, provided the problem can be reduced to a two-dimensional form, figures 2, 3, and 4, or,

$$\frac{\partial \Pi}{\partial \phi}=0. \tag{6}$$

The radio problem treated in this paper is one such two-dimensional problem.

2.1. Primary Field

The model for the source or transmitter is specified by the primary Hertz vector,

$$\Pi_0^e=I_0 l\left[\frac{\mu_0 c}{4\pi}\right]\frac{\exp\left[i\omega t-ik_1 D\right]}{-ik_1 D}, \tag{7}$$

where, for purposes of calculations, the source dipole current-moment, $I_o l$ ampere-meters, is taken as $I_0 l=\frac{4\pi}{\mu_0 c}\sim 3.34(10^{-2})$ ampere-meters. The radiation field of such a transmitter can be written approximately,

$$E_r\sim 10^{-7} I_0 l\,\frac{\omega}{D}\sin\theta\exp\left[i\omega t-ik_1 D\right] \tag{8}$$

or, over an infinitely conducting plane of infinite extent, figure 1, xy-plane:

$$E_r=E_z\sim 2(10^{-7}) I_0 l\,\frac{\omega}{D}\exp\left[i\omega t-ik_1 D\right]. \tag{9}$$

The radiation field is not necessarily the most important field at long wavelengths. Thus, unless the distance, D, is very great, the induction and electrostatic fields are quite important. It is therefore necessary to employ the exact expression for the assumed Hertz vector for the fields based on the Hertz vector (7), and eq (5),

$$E_r=\frac{-1}{rb\sin\theta}\left[\sin\theta\,\frac{\partial^2\Pi}{\partial\theta^2}+\cos\theta\,\frac{\partial\Pi}{\partial\theta}\right] \tag{10}$$

where $\Pi=\Pi_0^e$, or for the particular case of transmitter and receiver located on the surface of the sphere, $r=b=a$, figures 2, 3, and 4,

$$E_r=\frac{-1}{a^2}\left[\frac{\partial^2\Pi}{\partial\theta^2}+\frac{\cos\theta}{\sin\theta}\,\frac{\partial\Pi}{\partial\theta}\right]_{(r=b=a)}, \tag{11}$$

$$E_r=\frac{-1}{a^2}\exp\left[+i\omega t-ik_1 D\right]\left\{-\frac{1}{4}-\frac{\cos^2\frac{\theta}{2}}{\sin^2\frac{\theta}{2}}+\frac{\cos\theta}{4\sin^2\frac{\theta}{2}}+i\left[\frac{1}{8k_1 a\sin^3\frac{\theta}{2}}-\frac{k_1 a\cos^2\frac{\theta}{2}}{2\sin\frac{\theta}{2}}-\frac{\cos\theta}{4k_1 a\sin^2\frac{\theta}{2}}\right]\right\}. \tag{12}$$

The particular case, $\theta=\pi$, figures 2, 3, and 4, is of interest,

$$E_r=\frac{1}{a^2}\exp\left[i\omega t-2ik_1 a\right]\left[\frac{1}{2}-i\,\frac{3}{8k_1 a}\right], \tag{13}$$

since the transmitting and receiving dipoles are located end-to-end. The radiation field is therefore zero, but the induction and electrostatic fields remain finite and indeed not negligible

at extra low frequencies. However, at frequencies greater than, say, one kilocycle,

$$E_r \sim \frac{1}{2a^2} \exp\left[-2ik_1 a\right]_{(f>1\text{kc/s})}. \tag{14}$$

Similarily, the horizontal magnetic, H_ϕ, field can be written,

$$H_\phi = \frac{k_1^2}{\mu_0 i\omega a} \exp\left[i\omega t - ik_1 D\right] \left[\frac{\cos\frac{\theta}{2}}{2\sin\frac{\theta}{2}}\right] \left[1 - \frac{i}{2k_1 a \sin\frac{\theta}{2}}\right]_{(r=b=a)} \tag{15}$$

which for the particular case, $\theta=\pi$,

$$H_\phi = 0(\theta=\pi). \tag{16}$$

2.2. Media of Propagation

The media of propagation, figures 2, 3, and 4, are characterized by their electrical constants which can be expressed in concise form as the wave number, k. Thus, for air, with index of refraction, η, or dielectric constant $\epsilon_1, = \eta_1^2$,

$$k^2 = k_1^2 = \frac{\omega^2}{c^2} \epsilon_1, \tag{17}$$

or

$$k_1 \frac{\omega}{c} \eta_1, \tag{18}$$

($\epsilon_1 \sim 1.000676$ at the surface of the earth, $\epsilon_1 = 1$ in a vacuum, $\eta_1 \sim 1.000338$ at the surface of the earth, $\eta_1 = 1$ in a vacuum), where c is the speed of light, $c \sim 3(10^8)$ m/sec. ($c \sim 2.997925$ (10^8) m/sec in a vacuum.)

The angular wave number of the ground,

$$k = k_2 = \frac{\omega}{c} \sqrt{\epsilon_2 - i\,\frac{\sigma\mu_0 c^2}{\omega}}, \tag{19}$$

where σ is the ground conductivity and ϵ_2 is the relative dielectric constant (relative to a vacuum), where the permittivity, $\epsilon = \epsilon_2 \epsilon_0$, $\epsilon_0 = 1/c^2\ \mu_0$, and $\mu_0 = 4\pi$ (10^{-7}) h/m, the permeability of space.

The angular wave number of the ionosphere is more intricate,

$$k = k_3 = \frac{\omega}{c} \eta_{0,e}^{i,r}. \tag{20}$$

Thus, there are four distinct propagation components with the complex index of refraction' $\eta_{0,e}^{i,r}$ corresponding to ordinary wave (0), and extraordinary wave (e), upgoing wave (i), and downgoing wave (r). The index of refraction of the electron-ion plasma can be introduced with the plane coordinate system, figure 1. A simultaneous solution of Maxwell's eq (3) together with the Langevin equation of motion of the electron,

$$m\frac{d\overline{V}}{dt} + mg\overline{V} + \mu_0 e(\overline{V} \times \overline{H}_m) + e\overline{E} = 0, \tag{21}$$

where m is the mass of the electron, e is the electron charge, t is time, $\overline{V}$ is the vector velocity,

and $\overline{H}_m$ is the earth's static magnetic field vector, figure 1. Collisions of electrons with ions can be treated either from the viewpoint of classical magneto-ionic theory where $g \sim \nu$ and ν is a constant average value collision frequency, or from the more accurate Boltzmann theory of ionized gases in which electron collisions are proportional to energy, u, $\nu = \nu(u)$ [Phelps, 1960] where $g = g(\omega + \omega_H)$, $g(\omega - \omega_H)$, $g(\omega)$ [Johler and Harper, 1962] for a gyrofrequency, ω_H, or the parameter g is complex and frequency-dependent.

Carrying out the simultaneous solution of the Langevin equations together with Maxwell's equations results in a Booker [1939] type quartic in the parameter, ζ, assuming the convection currents, eq (3),

$$\overline{J} = -Ne\overline{V}, \tag{22}$$

or,

$$a_4\zeta^4 + a_3\zeta^3 + a_2\zeta^2 + a_1\zeta + a_0 = 0, \tag{23}$$

where the index of refraction, η,

$$\eta^2 = \zeta^2 + \sin^2 \phi_i, \tag{24}$$

and ϕ_i, figure 1, is the angle of incidence on the lower ionosphere plasma, and the coefficients a_4, a_3, a_2, a_1, a_0 are given in the appendix. The quartic (13) has four roots corresponding to four propagation components of the index of refraction (24), $\eta_{0,e}^{i,r}$. In special case of a single concentric, uniform plasma illustrated, figure 3, only the upgoing indexes, $\eta_{0,e}^{i}$, are of concern. The downgoing waves usually result from higher level reflections and correspond to the indexes $\eta_{0,e}^{r}$, figure 4.

The validity of the Q–L approximation [Budden, 1951] at long wavelengths has been checked numerically [Johler and Walters, 1960],

$$n_{0,e}^2 = 1 - i\frac{\omega_r}{\omega} \exp\left[\pm i\beta_1\right], \tag{25}$$

where

$$\tan \beta_1 = \frac{\omega_H}{\nu}, \tag{26}$$

$$\text{and } \frac{\omega_r}{\omega} = \frac{{\omega_N}^2}{\omega\sqrt{\nu^2 + {\omega_H}^2}}, \tag{27}$$

where ω_H and ω_N are the gyro and plasma frequencies defined in the appendix and ν is the constant classical collision frequency. The plus (+) sign is taken for the ordinary component, and the minus (−) sign is taken for the extraordinary component.

2.3. Heavy Ions

The effect of the heavy ions, i.e., the effect other than the collisions with electrons, cannot in general be neglected at extra low and ultra low radiofrequencies, since the gyrofrequency is approximately 50 c/s for these ions, according to Ratcliffe [1959]. An approach to this problem has been introduced by Pfister [1955]. This approach can be developed as a modification of the calculation of the index of refraction, η, of the plasma, but the formulation becomes quite intricate.

The number of positive ions, N_+, the number of negative ions, N_-, in addition to the number of electrons, $N = N_e$ are to be considered. The convection current components are, figure 1 eq (22):

$$\begin{aligned}
J_x &= -NeV_x = -e[N_eV_e{}^x - N_+V_+{}^x + N_-V_-{}^x] = J_x{}^e + J_x{}^+ + J_x{}^- \\
J_y &= -NeV_y = -e[N_eV_e{}^y - N_+V_+{}^y + N_-V_-{}^y] = J_y{}^e + J_y{}^+ + J_y{}^- \\
J_z &= -NeV_z = -e[N_eV_e{}^z - N_+V_+{}^z + N_-V_-{}^z] = J_z{}^e + J_z{}^+ + J_z{}^-.
\end{aligned} \tag{28}$$

The classical magneto-ionic collision frequency types, (ν can be described in connection with certain constants, C_1, C_2, C_3, . . .,

$$
\begin{aligned}
&C_1=\nu_{e,0}\frac{m_0}{m_e+m_0},\quad C_4=\nu_{+,0}\frac{m_0}{m_++m_0},\quad C_7=\nu_{-,0}\frac{m_0}{m_-+m_0},\quad C_{10}=\nu_{0,-}\frac{m_-}{m_0+m_-},\\
&C_2=\nu_{e,-}\frac{m_-}{m_e+m_-},\quad C_5=\nu_{+,-}\frac{m_-}{m_++m_-},\quad C_8=\nu_{-,+}\frac{m_+}{m_-+m_+},\quad C_{11}=\nu_{0,+}\frac{m_+}{m_0+m_+},\\
&C_3=\nu_{e,+}\frac{m_+}{m_e+m_+},\quad C_6=\nu_{+,e}\frac{m_e}{m_++m_e},\quad C_9=\nu_{-,e}\frac{m_e}{m_-+m_e},\quad C_{12}=\nu_{0,e}\frac{m_e}{m_0+m_e},
\end{aligned}
\tag{29}
$$

where $\nu_{e,0}$ is the electron-neutral molecule average collision frequency, $\nu_{e,-}$ is an electron-negative ion average collision frequency, etc., where the average velocity of like particles is assumed to be zero, and m_0, m_0, m_+, m_- are the masses of the neutral molecules, electrons, positive and negative ions respectively. The components of the Langevin eq (21) can then be written (assuming the Langevin equation can be applied to such ions),

$$i\omega V_{e,x}+\frac{e}{m_e}E_x+\frac{\mu_0 e}{m_e}[V_{e,y}H_{m,z}-V_{e,z}H_{m,y}]+(C_1+C_2+C_3)V_{e,x}-C_1V_{0,x}-C_2V_{-,x}-C_3V_{+,x}=0$$

$$i\omega V_{e,y}+\frac{e}{m_e}E_y+\frac{\mu_0 e}{m_e}[V_{e,z}H_{m,x}-V_{e,x}H_{m,z}]+(C_1+C_2+C_3)V_{e,y}-C_1V_{0,y}-C_2V_{-,y}-C_3V_{+,y}=0$$

$$i\omega V_{e,z}+\frac{e}{m_e}E_z+\frac{\mu_0 e}{m_e}[V_{e,x}H_{m,y}-V_{e,y}H_{m,x}]+(C_1+C_2+C_3)V_{e,z}-C_1V_{0,z}-C_2V_{-,z}-C_3V_{+,z}=0$$

$$i\omega V_{+,x}+\frac{-e}{m_+}E_x+\frac{-\mu_0 e}{m_+}[V_{+,y}H_{m,z}-V_{+,z}H_{m,y}]+(C_4+C_5+C_6)V_{+,x}-C_4V_{0,x}-C_5V_{-,x}-C_6V_{e,x}=0$$

$$i\omega V_{+,y}+\frac{-e}{m_+}E_y+\frac{-\mu_0 e}{m_+}[V_{+,z}H_{m,x}-V_{+,x}H_{m,z}]+(C_4+C_5+C_6)V_{+,y}-C_4V_{0,y}-C_5V_{-,y}-C_6V_{e,y}=0$$

$$i\omega V_{+,z}+\frac{-e}{m_+}E_z+\frac{-\mu_0 e}{m_+}[V_{+,x}H_{m,y}-V_{+,y}H_{m,x}]+(C_4+C_5+C_6)V_{+,z}-C_4V_{0,z}-C_5V_{-,z}-C_6V_{e,z}=0$$

$$i\omega V_{-,x}+\frac{e}{m_-}E_x+\frac{\mu_0 e}{m_-}[V_{-,y}H_{m,z}-V_{-,z}H_{m,y}]+(C_7+C_8+C_9)V_{-,x}-C_7V_{0,x}-C_8V_{+,x}-C_9V_{e,x}=0$$

$$i\omega V_{-,y}+\frac{e}{m_-}E_y+\frac{\mu_0 e}{m_-}[V_{-,z}H_{m,x}-V_{-,x}H_{m,z}]+(C_7+C_8+C_9)V_{-,y}-C_7V_{0,y}-C_8V_{+,y}-C_9V_{e,y}=0$$

$$i\omega V_{-,z}+\frac{e}{m_-}E_z+\frac{\mu_0 e}{m_-}[V_{-,x}H_{m,y}-V_{-,y}H_{m,x}]+(C_7+C_8+C_9)V_{-,z}-C_7V_{0,z}-C_8V_{+,z}-C_9V_{e,z}=0$$

$$
\begin{aligned}
&(C_{10}+C_{11}+C_{12})V_{0,x}-C_{10}V_{-,x}-C_{11}V_{+,x}-C_{12}V_{e,x}=0\\
&(C_{10}+C_{11}+C_{12})V_{0,y}-C_{10}V_{-,y}-C_{11}V_{+,y}-C_{12}V_{e,y}=0\\
&(C_{10}+C_{11}+C_{12})V_{0,z}-C_{10}V_{-,z}-C_{11}V_{+,z}-C_{12}V_{e,z}=0,
\end{aligned}
\tag{30}
$$

where the components, figure 1, of $\overline{E}$, and the velocity components of $\overline{V}$ are designated by the subscripts x, y, z of the plane local coordinate system at the ionosphere boundary.

The simultaneous solution of these eqs (30) with Maxwell's eqs (3) utilizing eq (28) results in two coupled matrix equations:

$$\begin{bmatrix} a_{11} & a_{12} & a_{13} & a_{14} & 0 & 0 & a_{17} & 0 & 0 \\ a_{21} & a_{22} & a_{23} & 0 & a_{25} & 0 & 0 & a_{28} & 0 \\ a_{31} & a_{32} & a_{33} & 0 & 0 & a_{36} & 0 & 0 & a_{39} \\ a_{41} & 0 & 0 & a_{44} & a_{45} & a_{46} & a_{47} & 0 & 0 \\ 0 & a_{52} & 0 & a_{54} & a_{55} & a_{56} & 0 & a_{58} & 0 \\ 0 & 0 & a_{63} & a_{64} & a_{65} & a_{66} & 0 & 0 & a_{69} \\ a_{71} & 0 & 0 & a_{74} & 0 & 0 & a_{77} & a_{78} & a_{79} \\ 0 & a_{82} & 0 & 0 & a_{85} & 0 & a_{87} & a_{88} & a_{89} \\ 0 & 0 & a_{93} & 0 & 0 & a_{96} & a_{97} & a_{98} & a_{99} \end{bmatrix} \cdot \begin{bmatrix} J_x^e \\ J_y^e \\ J_z^e \\ J_x^+ \\ J_y^+ \\ J_z^+ \\ J_x^- \\ J_y^- \\ J_z^- \end{bmatrix} + \begin{bmatrix} E_x \\ E_y \\ E_z \\ E_x \\ E_y \\ E_z \\ E_x \\ E_y \\ E_z \end{bmatrix} = 0 \qquad (31)$$

and

$$\begin{bmatrix} b_{11} & b_{12} & b_{13} \\ b_{21} & b_{22} & b_{23} \\ b_{31} & b_{32} & b_{33} \end{bmatrix} \cdot \begin{bmatrix} E_x \\ E_y \\ E_z \end{bmatrix} + \begin{bmatrix} C(J_x^e + J_x^+ + J_x^-) \\ C(J_y^e + J_y^+ + J_y^-) \\ C(J_z^e + J_z^+ + J_z^-) \end{bmatrix} = 0, \qquad (32)$$

where $C = -1/i\omega\epsilon_0$, and the a_{ij} and b_{ij} are defined in the appendix.

The two eqs (31, 32) are equivalent to the single equation,

$$\left[\begin{array}{ccccccccc:ccc} a_{11} & a_{12} & a_{13} & a_{14} & 0 & 0 & a_{17} & 0 & 0 & 1 & 0 & 0 \\ a_{21} & a_{22} & a_{23} & 0 & a_{25} & 0 & 0 & a_{28} & 0 & 0 & 1 & 0 \\ a_{31} & a_{32} & a_{33} & 0 & 0 & a_{36} & 0 & 0 & a_{39} & 0 & 0 & 1 \\ a_{41} & 0 & 0 & a_{44} & a_{45} & a_{46} & a_{47} & 0 & 0 & 1 & 0 & 0 \\ 0 & a_{52} & 0 & a_{54} & a_{55} & a_{56} & 0 & a_{58} & 0 & 0 & 1 & 0 \\ 0 & 0 & a_{63} & a_{64} & a_{65} & a_{66} & 0 & 0 & a_{69} & 0 & 0 & 1 \\ a_{71} & 0 & 0 & a_{74} & 0 & 0 & a_{77} & a_{78} & a_{79} & 1 & 0 & 0 \\ 0 & a_{82} & 0 & 0 & a_{85} & 0 & a_{87} & a_{88} & a_{89} & 0 & 1 & 0 \\ 0 & 0 & a_{93} & 0 & 0 & a_{96} & a_{97} & a_{98} & a_{99} & 0 & 0 & 1 \\ \hdashline C & 0 & 0 & C & 0 & 0 & C & 0 & 0 & b_{11} & b_{12} & b_{13} \\ 0 & C & 0 & 0 & C & 0 & 0 & C & 0 & b_{21} & b_{22} & b_{23} \\ 0 & 0 & C & 0 & 0 & C & 0 & 0 & C & b_{31} & b_{32} & b_{33} \end{array}\right] \cdot \begin{bmatrix} J_x^e \\ J_y^e \\ J_z^e \\ J_x^+ \\ J_y^+ \\ J_z^+ \\ J_x^- \\ J_y^- \\ J_z^- \\ E_x \\ E_y \\ E_z \end{bmatrix} = 0. \qquad (33)$$

The 12 × 12 matrix, eq (33), and the vector submatrices can be divided into block matrices as indicated by the dashed line,

$$\begin{bmatrix} M_{9\times9} & N_{9\times3} \\ P_{3\times9} & Q_{3\times3} \end{bmatrix} \begin{bmatrix} J_{9\times1} \\ K_{3\times1} \end{bmatrix} = 0. \qquad (34)$$

Then
$$M \cdot J + N \cdot K = 0. \tag{35}$$

and
$$P \cdot J + Q \cdot K = 0. \tag{36}$$

If M^{-1} exists, multiply eq (35) by $P \cdot M^{-1}$ and subtract from eq (36). Then,

$$Q \cdot K - P \cdot M^{-1} \cdot N \cdot K = (Q - P \cdot M^{-1} \cdot N) \cdot K = 0. \tag{37}$$

But,

$$Q = \begin{bmatrix} b_{11} & b_{12} & b_{13} \\ b_{21} & b_{22} & b_{23} \\ b_{31} & b_{32} & b_{33} \end{bmatrix}, \text{ and } K = \begin{bmatrix} E_x \\ E_y \\ E_z \end{bmatrix}$$

and $P \cdot M^{-1} \cdot N$ can be computed numerically [Johler and Harper, 1962; Johler and Walters, 1960]. Thus $(Q - P \cdot M^{-1} \cdot N)$ can be written as a matrix involving the complex number, ζ, eqs (23, 24). $(Q - P \cdot M^{-1} \cdot N) \cdot K = 0$ has a nontrivial solution if, and only if, $|Q - P \cdot M^{-1} \cdot N| = 0$. This yields a polynomial in ζ which can be solved to find ζ [Johler and Walters, 1960]. These results depend on the existence of M^{-1} where M is the original 9×9 matrix, eq (31). If E exists, the nonexistence of M^{-1} would imply that eq (31) has no unique solution.

Writing,

$$\begin{vmatrix} b_{11} - \alpha_{11} & b_{12} - \alpha_{12} & b_{13} - \alpha_{13} \\ b_{21} - \alpha_{21} & b_{22} - \alpha_{22} & b_{23} - \alpha_{23} \\ b_{31} - \alpha_{31} & b_{32} - \alpha_{32} & b_{33} - \alpha_{33} \end{vmatrix} = \left| Q - P \cdot M^{-1} \cdot N \right| = 0, \tag{38}$$

and letting (see appendix for $a_L a_T$)

$$\begin{aligned} a &= a_L^2 - 1 - \alpha_{11} & g &= -a_L \\ b &= -a_L a_T - \alpha_{12} & h &= -\alpha_{23} \\ c &= -a_T & i &= -a_T \\ d &= -\alpha_{13} & j &= -\alpha_{31} \\ e &= -a_T a_L - \alpha_{21} & k &= a_L a_T - \alpha_{32} \\ f &= a_T^2 - 1 - \alpha_{22} & l &= a_T^2 + a_T a_L - 1 - \alpha_{33}, \end{aligned} \tag{39}$$

then eq (38) becomes,

$$\begin{vmatrix} \zeta^2 + a & b & c\zeta + d \\ e & \zeta^2 + f & g\zeta + h \\ i\zeta + j & k & l \end{vmatrix} =$$

$$\zeta^4(l - ic) + \zeta^3(-cj - id - kg) + \zeta^2(la + lf + bgi - fic - jd - kh) + \zeta(bhi + bjg + ekc - fcj - idf - kag) + (afl + bhj + ekd - fjd - kha - lbe), \tag{40}$$

or,

$$\begin{vmatrix} \zeta^2 + a & b & c\zeta + d \\ e & \zeta^2 + f & g\zeta + h \\ i\zeta + j & k & l \end{vmatrix} = a_4\zeta^4 + a_3\zeta^3 + a_2\zeta^2 + a_1\zeta + a_0 \tag{41}$$

where,

$$\begin{aligned} a_3 &= l - a_T^2 \\ a_3 &= a_T\alpha_{31} - a_T\alpha_{13} + ka_L \\ a_2 &= la + lf + ba_L a_T - a_T^2 - \alpha_{13}\alpha_{31} + k\alpha_{23} \\ a_1 &= ba_T\alpha_{23} + ba_L\alpha_{31} - eka_T - fa_T\alpha_{31} - fa_T\alpha_{13} + kaa_L \\ a_0 &= afl + b\alpha_{23}\alpha_{31} - ek\alpha_{13} - f\alpha_{31}\alpha_{13} + ka\alpha_{23} - lbe. \end{aligned} \tag{42}$$

A preliminary numerical evaluation of the eqs (28–42) based on estimated approximate values of collision frequency and ion density indicated ion gyrofrequencies which could affect the index of refraction at long wavelengths (1 c/s to 100 c/s).

2.4. Boundary Conditions

The conventional procedure for the solution of electromagnetic-wave propagation problems requires the description of the propagation in the various media assuming each of these to be of infinite extent in space. Thus, figures 2, 3, and 4, the electromagnetic wave is determined by the wave equation in the Hertz vector and the angular-wave number,

$$\begin{aligned}(\nabla^2+k_1^2)\Pi&=0\\(\nabla^2+k_2^2)\Pi&=0\\(\nabla^2+k_3^2)\Pi&=0\\&\ldots,\end{aligned}\tag{43}$$

where the arabic numeral subscripts, 1, 2, 3, distinguish the three media of propagation described by the wave numbers k_1, k_2, k_3. The boundaries $r=a$, c . . ., figures 2, 3, and 4, are then introduced by equating the tangential $\overline{E}$ and $\overline{H}$ fields and perhaps the normal $\overline{H}$ fields immediately on each side of each boundary such that these fields are continuous across the boundary.

The boundary conditions for the particular example, figure 3, comprising a finitely-conducting sphere, a concentric plasma shell of infinite extent and uniform composition will now be considered in detail. The tangential components of $\overline{E}$ and $\overline{H}$ fields, eq (5) derived from appropriate Hertz vectors, $\Pi_{1,2,3}$ for the various media are equated at the boundaries. The medium of wave number, k_3 is a magneto-ionic medium involving ordinary and extraordinary wave numbers $k_{3,0}$, $k_{3,e}$ which can be treated as constants so that the wave eq (43) and corresponding Hertz vectors, $\Pi_{3,0}$, $\Pi_{3,e}$, can be used (see appendix). The distinction between the two upgoing (i) propagation components and the downgoing (r) propagation components is not necessary in this case since the medium of wave number k_3 is of infinite extent. Downgoing waves arise from additional boundaries such as those illustrated, figure 4. The boundary conditions [Stratton, 1941] can be written by expressing the equality of the tangential components of the field on each side and in the immediate vicinity of the boundary,

$$\begin{aligned}H_{\phi,1}&=H_{\phi,3(0,e)}\\E_{\phi,1}&=E_{\phi,3(0,e)}\\E_{\theta,1}&=E_{\theta,3(0,e)}\\H_{\theta,1}&=H_{\theta,3(0,e)}\\H_{\phi,1}&=H_{\phi,2}\\E_{\phi,1}&=E_{\phi,2}\\H_{\theta,1}&=H_{\theta,2}\\E_{\theta,1}&=E_{\theta,2}\end{aligned}\tag{44}$$

Straightforward substitution of eqs (5) into (44) would result in two sets of uncoupled equations for the electrical and magnetical solutions. Therefore, it is necessary to define the coupling in accordance with certain rules of the magneto-ionic theory. This can be accomplished with the $Q-L$ approximation [Johler and Walters, 1960],

$$\frac{Q_0\zeta_0}{\eta_0}\sim i, \qquad P_0\sim\frac{-\sin\phi_i}{\eta_0\cos\theta_0}\tag{45}$$

$$\frac{Q_e\zeta_e}{\eta_e}\sim -i, \qquad P_e\sim\frac{-\sin\phi_i}{\eta_e\cos\theta_e},\tag{46}$$

where $\sin\phi_i=\eta\sin\theta$, and Q_0, Q_e are the ordinary and extraordinary components of $-Q_{me}$ and where the rectangular cartesian coordinates are related locally at the model ionosphere boundary

to the spherical components,

$$-Q_{me}=\frac{E_x}{E_y}=-\frac{E_\phi}{E_\theta}, \qquad P_{me}=\frac{E_z}{E_y}=\frac{E_r}{E_\theta}=\frac{-\sin\phi_i}{\zeta}, \tag{47}$$

or,

$$E_\phi=Q_{me}E_\theta\sim\mp i\frac{\eta}{\zeta}E_\theta$$

$$E_r=P_{me}E_\theta\sim\frac{-\sin\phi_i}{\zeta}E_\theta \tag{48}$$

$$H_\theta=Q_{em}H_\phi,$$

$$H_r=P_{em}H_\phi. \tag{49}$$

The coupling can be introduced into the boundary conditions by writing

$$E_{\phi,1}=QE_{\theta,3} \tag{50}$$

at $r=c$. Equation (50), and the equated tangential fields, eq (44), can be written in terms of the Hertz vector Π, assuming a vertical electric dipole transmitter, $\vec{r}\,\Pi_0^e$ located in medium of wave number k_1,

$$\left[\begin{array}{c} k_1^2(\Pi_0^e+\Pi_1^e)=k_2^2(\Pi_2^e) \\ \frac{\partial}{\partial r}(r\Pi_0^e+r\Pi_1^e)=\frac{\partial}{\partial r}(r\Pi_2^e) \\ \Pi_1^m=\Pi_2^m \\ \frac{\partial}{\partial r}(r\Pi_1^m)=\frac{\partial}{\partial r}(r\Pi_2^m) \end{array}\right]_{r=a} \tag{51}$$

$$\left[\begin{array}{l} k_1^2(\Pi_0^e+\Pi_1^e)=\mu_0 i\omega Q_{em}^{-1}\frac{1}{r}\frac{\partial}{\partial r}(r\Pi_3^m) \\ \frac{1}{r}\frac{\partial}{\partial r}(r\Pi_0^e+r\Pi_1^e)=\mu_0 i\omega Q_{me}^{-1}\Pi_3^m \\ \Pi_1^m=Q_{me}\frac{1}{r}\frac{\partial}{\partial r}(r\Pi_3^e) \\ \mu_0 i\omega\frac{\partial}{\partial r}(r\Pi_1^m)=Q_{em}k_3^2\Pi_3^e \end{array}\right]_{r=c} \tag{52}$$

where in the Q-L approximation,

$$Q_{me}=\pm i\left[\frac{k_3/k_1}{\sqrt{k_3^2/k_1^2-\rho}}\right], \; P_{me}=\frac{-\sin\phi_i}{\zeta},$$

and $\rho=\sin^2\phi_2$ is the complex direction sine squared of propagation, and the minus sign (—) is taken with the ordinary wave, $k_{3,0}$, and the plus (+) sign is taken with the extraordinary wave $k_{3,e}$.

The quantity ρ, for the case of a plane wave incident upon the ionosphere, can be identified with a local angle of incidence, ϕ_i, at the model ionosphere boundary.

$$\rho=\sin^2\phi_i. \tag{53}$$

However, in the case of the spherical waves incident on the ionosphere at $r=$c,

$$\sin^2\phi_i=\left[1+\left(\frac{E_{\theta,n}}{E_{r,n}}\right)^2\right]^{-1}\sim\frac{n^2}{k^2c^2} \tag{54}$$

a complex angle of incidence, which can be written explicitly for each spherical wave ζ_n, ψ_n, as shown in the appendix.

The solution of the wave eq (43) when $\frac{\partial \Pi}{\partial \phi}=0$,

$$\frac{1}{r^2}\frac{\partial}{\partial r}\left[r^2\frac{\partial \Pi}{\partial r}\right]+\frac{1}{r^2\sin\theta}\frac{\partial}{\partial\theta}\left[\sin\theta\frac{\partial \Pi}{\partial\theta}\right]+k^2\Pi=0 \tag{55}$$

depends upon the separation of variables, θ and r,

$$\Pi=f(r)F(\theta), \tag{56}$$

whereupon,

$$\frac{-\frac{\partial}{\partial\theta}\left[\sin\theta\frac{\partial}{\partial\theta}F(\theta)\right]}{F(\theta)\sin\theta}=\lambda=\frac{\frac{\partial}{\partial r}\left[r^2\frac{\partial}{\partial r}f(r)\right]+k^2r^2f(r)}{f(r)} \tag{57}$$

in which Legendre differential equation is satisfied by the Legendre function,

$$F(\theta)=P_n(\cos\theta), \tag{58}$$

where,

$$P_0(\cos\theta)=1,$$

$$P_1(\cos\theta)=\cos\theta,$$

$$P_2(\cos\theta)=\tfrac{1}{2}(3\cos^2\theta-1),$$

$$P_3(\cos\theta)=\tfrac{1}{2}(5\cos^3\theta-3\cos\theta),$$

$$\cdots$$

and the eigenva ues,

$$\lambda=n(n+1),$$

$$n=0, 1, 2, 3, \ldots, \tag{59}$$

or,

$$(1-z^2)\frac{d^2P_n(z)}{dz^2}-2z\frac{dP_n(z)}{dz}+n(n+1)P_n(z)=0, \tag{60}$$

where $z=\cos\theta$.

Also, eq (57) [Stratton, 1941], since

$$\frac{1}{r^2}\frac{\partial}{\partial r}\left[r^2\frac{\partial f}{\partial r}\right]=\frac{1}{r}\frac{\partial^2}{\partial r^2}[rf],$$

$$\frac{d^2z}{d\xi^2}+\frac{1}{\xi}\frac{dz}{d\xi}+\left[1-\frac{(n+\frac{1}{2})^2}{\xi^2}\right]z=0, \tag{61}$$

where $z=\sqrt{\xi f(r)}$, $\xi=kr$, which is Bessel's equation.

Thus, the solution of eq (55) can be written as a series of zonal harmonics consisting of terms of the form $(\beta_n\psi_n(kr)+\gamma_n\zeta_n(kr))\times P_n(\cos\theta)$, where β_n and γ_n are constants and

$$\psi_n(z)=\sqrt{\frac{\pi z}{2}}J_{n+\frac{1}{2}}(z), \tag{62}$$

$$\zeta_n(z)=\sqrt{\frac{\pi z}{2}}H^{(2)}_{n+\frac{1}{2}}(z), \tag{63}$$

$J_{n+1/2}(z)$ and $H^{(2)}_{u}{}_{+1/2}(z)$ are Bessel and Hankel functions (solutions of eq (61)) of order $n+1/2$ and argument z and the Hankel function $H^{(2)}$ is of the second kind [Watson, 1958]. The ζ-waves

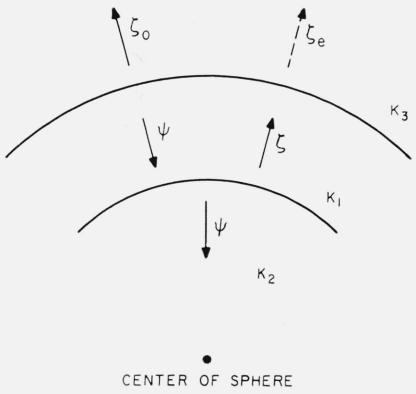

FIGURE 5. *Terrestrial sphere cross section with concentric plasma illustrating various types of progressing spherical waves in the three media of propagation.*
Outgoing ζ-waves and ingoing ψ-waves.

vanish at $r=\infty$, figure 5, and the ψ-waves vanish at $r=0$. In particular,

$$\Pi_0^e=\frac{1}{k_1^2rb}\sum_{n=0}^{\infty}(2n+1)\zeta_n(k_1b)\psi_n(k_1r)P_n(\cos\theta),\ (r<b)$$

$$=\frac{1}{k_1^2rb}\sum_{n=0}^{\infty}(2n+1)\zeta_n(k_1r)\psi_n(k_1b)P_n(\cos\theta),\ (r>b) \tag{64}$$

$$\Pi_1^e=\frac{1}{k_1^2rb}\sum_{n=0}^{\infty}(2n+1)[b_n^e\zeta_n(k_1r)+c_n^e\psi_n(k_1r)]P_n(\cos\theta) \tag{65}$$

$$\Pi_1^m=\frac{1}{k_1^2rb}\sum_{n=0}^{\infty}(2n+1)[b_n^m\zeta_nk_1r)+c_n^m\zeta_n(k_1r)]P_n(\cos\theta) \tag{66}$$

$$\Pi_2^e=\frac{1}{k_2^2rb}\sum_{n=0}^{\infty}(2n+1)a_n^e\psi_n(k_2r)P_n(\cos\theta), \tag{67}$$

$$\Pi_2^m=\frac{1}{k_2^2rb}\sum_{n=0}^{\infty}(2n+1)a_n^m\psi_n(k_2r)P_n(\cos\theta), \tag{68}$$

$$\Pi_3^e=\frac{1}{k_3^2rb}\sum_{n=0}^{\infty}(2n+1)d_n^e\zeta_n(k_3r)P_n(\cos\theta), \tag{69}$$

$$\Pi_3^m=\frac{1}{k_3^2rb}\sum_{n=0}^{\infty}(2n+1)d_n^m\zeta_n(k_3r)P_n(\cos\theta). \tag{70}$$

The subscripts, 1, 2, 3, refer to the Hertz vector fields in the various media, figure 3, and a_n^e, b_n^e, etc., are constants determined by the boundary conditions, eq (71).

The boundary conditions, eqs (51, 52), can be written in concise form as the matrix equation:

$$\begin{bmatrix} a_{1,1} & a_{1,2} & a_{1,3} & 0 & 0 & 0 & 0 & 0 \\ a_{2,1} & a_{2,2} & a_{2,3} & 0 & 0 & 0 & 0 & 0 \\ 0 & a_{3,2} & a_{3,3} & 0 & 0 & 0 & 0 & a_{3,8} \\ 0 & a_{4,2} & a_{4,3} & 0 & 0 & 0 & 0 & a_{4,8} \\ 0 & 0 & 0 & a_{5,4} & 0 & a_{5,6} & a_{5,7} & 0 \\ 0 & 0 & 0 & 0 & a_{6,5} & a_{6,6} & a_{6,7} & 0 \\ 0 & 0 & 0 & 0 & a_{7,5} & a_{7,6} & a_{7,7} & 0 \\ 0 & 0 & 0 & a_{8,4} & 0 & a_{8,6} & a_{8,7} & 0 \end{bmatrix} \begin{bmatrix} a_n^e \\ b_n^e \\ c_n^e \\ d_n^e \\ a_n^m \\ b_n^m \\ c_n^m \\ d_n^m \end{bmatrix} = \begin{bmatrix} a_{1,0} \\ a_{2,0} \\ a_{3,0} \\ a_{4,0} \\ 0 \\ 0 \\ 0 \\ 0 \end{bmatrix} \tag{71}$$

where,

$$
\begin{aligned}
a_{1,0} &= -\zeta_n(k_1 b)\psi_n(k_1 a) & a_{4,3} &= \frac{1}{k_1}\psi_n'(k_1 c)\\
a_{1,1} &= -\psi_n(k_2 a) & a_{4,8} &= -\frac{-\mu_0 i\omega}{k_3^2 Q_{me}}\zeta_n(k_3 c)\\
a_{1,2} &= \zeta_n(k_1 a) & a_{5,4} &= -\frac{Q_{me}}{k_3^2}\zeta_n(k_3 c)\\
a_{1,3} &= \psi_n(k_1 a) & a_{5,6} &= \frac{\mu_0 i\omega}{k_1^2}\zeta_n(k_1 c)\\
a_{2,0} &= -\frac{1}{k_1}\zeta_n(k_1 b)\zeta_n'(k_1 a) & a_{5,7} &= \frac{1}{k_1^2}\psi_n(k_3 c)\\
a_{2,1} &= -\frac{1}{k_2}\psi_n'(k_2 a) & a_{6,5} &= \frac{-1}{k_2^2}\psi_n(k_2 a)\\
a_{2,2} &= \frac{1}{k_1}\zeta_n'(k_1 a) & a_{6,6} &= \frac{1}{k_1^2}\zeta_n(k_1 a)\\
a_{2,3} &= \frac{1}{k_1}\psi_n'(k_1 a) & a_{6,7} &= \frac{1}{k_1^2}\psi_n(k_1 a)\\
a_{3,0} &= -\zeta_n(k_1 c)\psi_n(k_1 b) & a_{7,5} &= -\frac{1}{k_2}\psi_n'(k_2 a)\\
a_{3,2} &= \zeta_n(k_1 c) & a_{7,6} &= \frac{1}{k_1}\zeta_n'(k_1 a)\\
a_{3,3} &= \psi_n(k_1 c) & a_{7,7} &= \frac{1}{k_1}\psi_n'(k_1 a)\\
a_{3,8} &= \frac{-\mu_0 i\omega}{k_3 Q_{em}}\zeta_n'(k_3 c) & a_{8,4} &= -Q_{em}\zeta_n(k_3 c)\\
a_{4,0} &= -\frac{1}{k_1}\zeta_n'(k_1 a)\psi_n(k_1 b) & a_{8,6} &= \frac{\mu_0 i\omega}{k_1}\psi_n'(k_1 c)\\
a_{4,2} &= \frac{1}{k_1}\zeta_n'(k_1 c) & a_{8,7} &= \frac{\mu_0 i\omega}{k_1}\zeta_n'(k_1 c).
\end{aligned}
\tag{72}
$$

Under certain conditions, such as long wavelengths [Johler and Walters, 1960; Johler, 1961; Johler, Walters, and Harper, 1960], the effect of coupling in the region between $r=a$ and $r=c$, figures 2, 3, and 4, can be neglected. This assumption reduces the matrix eq. (71) to,

$$
\begin{bmatrix}
-\psi_n(k_2 a) & \zeta_n(k_1 a) & \psi_n(k_1 a) & 0\\
-\frac{1}{k_2}\psi_n'(k_2 a) & \frac{1}{k_1}\zeta_n'(k_1 a) & \frac{1}{k_1}\psi_n'(k_1 a) & 0\\
0 & \zeta_n(k_1 c) & \psi_n(k_1 a) & [-\zeta_n(k_3 c)]\\
0 & \frac{1}{k_1}\zeta_n'(k_1 c) & \frac{1}{k_1}\psi_n'(k_1 c) & \left[-\frac{1}{k_3}\zeta_n'(k_3 c)\right]
\end{bmatrix}
\begin{bmatrix} a_n\\ b_n\\ c_n\\ d_n \end{bmatrix}
=
\begin{bmatrix}
-\zeta_n(k_1 b)\psi_n(k_1 a)\\
\frac{-1}{k_1}\zeta_n(k_1 b)\psi_n'(k_1 a)\\
-\zeta_n(k_1 c)\psi_n(k_1 b)\\
\frac{-1}{k_1}\zeta_n'(k_1 c)\psi_n(k_1 b)
\end{bmatrix}
\tag{73}
$$

where $a_n=a_n^e$, $bn=b_n^e$, $c_n=c_n^e$, $d_n=d_n^e$, $k_3=k_{3,0}$, $k_{3,e}$.

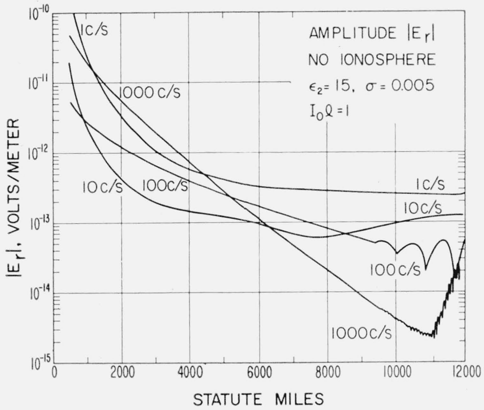

FIGURE 6. *Amplitude of the vertical electric field, $|E_r|$, of the ground wave excited by a vertical electric time harmonic dipole source current moment as a function of distance, d, along the surface of the terrestrial sphere, illustrating the standing wave at the antipode of the transmitter resulting from two waves traveling "around-the-world" in opposite directions.*

$$I_0 l = \frac{4\pi}{\mu_0 c} \sim 3.34(10^{-2})$$

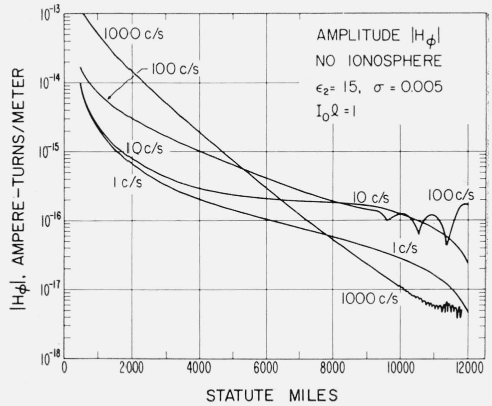

FIGURE 8. *Amplitude of the horizontal magnetic field, $|H_\phi|$, of the ground wave excited by a vertical electric dipole time-harmonic dipole source current moment as a function of the distance, d, along the surface of the terrestrial sphere, illustrating the standing wave near the antipode of the transmitter resulting from two waves traveling "around-the-world" in opposite directions.*

$$I_0 l = \frac{4\pi}{\mu_0 c} \sim 3.34(10^{-2})$$

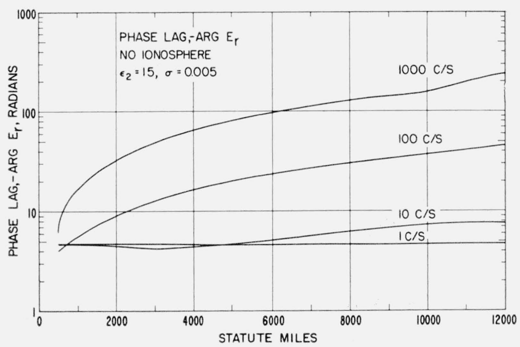

FIGURE 7. *Phase of the vertical electric field,* arg E_r, *of the ground wave.*

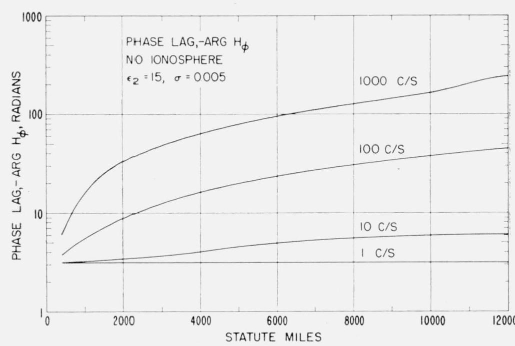

FIGURE 9. *Phase of the horizontal magnetic field,* arg H_ϕ, *of the ground wave.*

This matrix (eq. 73) can be generalized for straification of the sphere and the continuoulsy stratified concentric plasma,

$$\begin{bmatrix}
\chi_{1,1}\chi_{1,2}\chi_{1,3} \\
\chi_{2,1}\chi_{2,2}\chi_{2,3} \\
\quad \chi_{3,2}\chi_{3,3}\chi_{3,4}\chi_{3,5} \\
\quad \chi_{4,2}\chi_{4,3}\chi_{4,4}\chi_{4,5} \\
\qquad \chi_{5,4}\chi_{5,5}\chi_{5,6}\chi_{5,7} \\
\qquad \chi_{6,4}\chi_{6,5}\chi_{6,6}\chi_{6,7} \\
\qquad\quad \chi_{7,6}\chi_{7,7}\chi_{7,8}\chi_{7,9} \\
\qquad\quad \chi_{8,6}\chi_{8,7}\chi_{8,8}\chi_{8,9} \\
\qquad \cdots\cdots\cdots \\
\qquad\qquad \chi_{2m+3,2m+2}\chi_{2m+3,2m+3}\chi_{2m+3,2m+4}\chi_{2m+3,2m+5} \\
\qquad\qquad \chi_{2m+4,2m+2}\chi_{2m+4,2m+3}\chi_{2m+4,2m+4}\chi_{2m+4,2m+5} \\
\qquad\qquad \cdots\cdots\cdots\cdots\cdots\cdots \\
 \\
 \\
 \\
\qquad\qquad\qquad \chi_{2p+3,2p+2}\chi_{2p+3,2p+3}\chi_{2p+3,2p+4} \\
\qquad\qquad\qquad \chi_{2p+4,2p+2}\chi_{2p+4,2p+3}\chi_{2p+4,2p+4}
\end{bmatrix}
\begin{bmatrix}
a_{2,n} \\ f_{1,n} \\ a_{1,n} \\ b_n \\ c_n \\ d_{1,n} \\ e_{1,n} \\ d_{2,n} \\ \cdots \\ d_{m-1,n} \\ e_{m-1,n} \\ d_{m,n} \\ e_{m,n} \\ \cdots \\ d_{p-1,n} \\ e_{p-1,n} \\ d_{p,n}
\end{bmatrix}
=
\begin{bmatrix}
 \\ \\ \\ \chi_{3,0} \\ \chi_{4,0} \\ \chi_{5,0} \\ \chi_{6,0} \\ \\ \\ \\ \\ \\ \\ \\ \\ \\ \\
\end{bmatrix} \tag{74}$$

where

$$\chi_{1,1}=-\psi_n(k_{2,2}f) \qquad \chi_{4,4}=\frac{1}{k_1}\zeta'_n(k_1a)$$

$$\chi_{1,2}=\zeta_n(k_{2,1}f) \qquad \chi_{4,5}=\frac{1}{k_1}\psi'_n(k_1a)$$

$$\chi_{1,3}=\psi_n(k_{2,1}f) \qquad \chi_{5,0}=-\zeta_n(k_1c_1)\psi_n(k_1b)$$

$$\chi_{2,1}=-\frac{1}{k_{2,2}}\psi'_n(k_{2,2}f) \qquad \chi_{5,4}=\zeta_n(k_1c_1)$$

$$\chi_{2,2}=\frac{1}{k_{2,1}}\zeta'_n(k_{2,1}f) \qquad \chi_{5,5}=\psi_n(k_1c_1)$$

$$\chi_{2,3}=\frac{1}{k_{2,1}}\psi'_n(k_{2,1}f) \qquad \chi_{5,6}=-\zeta_n(k_{3,1}c_1)$$

$$\chi_{3,0}=-\zeta_n(k_1b)\psi_n(k_1a) \qquad \chi_{5,7}=-\psi_n(k_{3,1}c_1)$$

$$\chi_{3,2}=-\zeta_n(k_{2,1}a) \qquad \chi_{6,0}=-\frac{1}{k_1}\zeta'_n(k_1c_1)\psi_n(k_1b)$$

$$\chi_{3,3}=-\psi_n(k_{2,1}a) \qquad \chi_{6,4}=\frac{1}{k_1}\zeta'_n(k_1c_1)$$

$$\chi_{3,4}=\zeta_n(k_1a) \qquad \chi_{6,5}=\frac{1}{k_1}\psi'_n(k_1c_1)$$

$$\chi_{3,5}=\psi_n(k_1a) \qquad \chi_{6,6}=-\frac{1}{k_{3,1}}\zeta'_n(k_{3,1}c_1)$$

$$\chi_{4,0}=-\frac{1}{k_1}\zeta_n(k_1b)\psi'_n(k_1a) \qquad \chi_{6,7}=-\frac{1}{k_{3,1}}\psi'_n(k_{3,1}c_1)$$

$$\chi_{4,2}=-\frac{1}{k_{2,1}}\zeta'_n(k_{2,1}a) \qquad \chi_{7,6}=\zeta_n(k_{3,1}c_2)$$

$$\chi_{4,3}=-\frac{1}{k_{2,1}}\psi'_n(k_{2,1}a) \qquad \chi_{7,7}=\psi_n(k_{3,1}c_2)$$

$$\chi_{7,8}=-\zeta_n(k_{3,2}c_2)$$

$$\chi_{7,9}=-\psi_n(k_{3,2}c_2)$$

$$\chi_{8,6}=\frac{1}{k_{3,1}}\zeta'_n(k_{3,1}c_2)$$

$$\chi_{8,7}=\frac{1}{k_{3,1}}\psi'_n(k_{3,1}c_2)$$

$$\chi_{8,8}=-\frac{1}{k_{3,2}}\zeta'_n(k_{3,2}c_2)$$

$$\chi_{8,9}=-\frac{1}{k_{3,2}}\psi'_n(k_{3,2}c_2)$$

. . . .

$$\chi_{2m+4,2m+2}=\frac{1}{k_{3,m-1}}\zeta'_n(k_{3,m-1}c_m)$$

$$\chi_{2m+4,2m+3}=\frac{1}{k_{3,m-1}}\psi'_n(k_{3,m-1}c_m)$$

$$\chi_{2m+4,2m+4}=-\frac{1}{k_{3,m}}\zeta'_n(k_{3,m}c_m)$$

$$\chi_{2m+4,2m+5}=-\frac{1}{k_{3,m}}\psi'_n(k_{3,m}c_m)$$

. . . .

. . . .

$$\chi_{2p+3,2p+2}=\zeta_n(k_{3,p-1}c_p)$$

$$\chi_{2p+3,2p+3}=\psi_n(k_{3,p-1}c_p)$$

$$\chi_{2p+3,2p+4}=-\zeta_n(k_{3,p}c_p)$$

. . . .

$$\chi_{2m+3,2m+2}=\zeta_n(k_{3,m-1}c_m) \qquad \chi_{2p+4,2p+2}=\frac{1}{k_{3,p-1}}\zeta_n'(k_{3,p-1}c_p)$$

$$\chi_{2m+3,2m+3}=\psi_n(k_{3,m-1}c_m) \qquad \chi_{2p+4,2p+3}=\frac{1}{k_{3,p-1}}\psi_n'(k_{3,p-1}c_p)$$

$$\chi_{2m+3,2m+4}=-\zeta_n(k_{3,m}c_m)$$

$$\chi_{2m+3,2m+5}=-\psi_n(k_{3,m}c_m) \qquad \chi_{2p+4,2p+4}=\frac{-1}{k_{3,p}}\zeta_n'(k_{3,p}c_p). \tag{75}$$

The inner sphere, figure 4, has wave number $k_{2,2}$, radius f, and Hertz vector,

$$\Pi_{2,2}=\frac{1}{k_{2,2}^2 rb}\sum_{n=0}^{\infty}(2n+1)a_{2,n}\psi_n(k_{2,2}r)P_n(\cos\theta);$$

the outer layer of the earth has wave number $k_{2,1}$, radius a, and Hertz vector,

$$\Pi_{2,1}=\frac{1}{k_{2,1}^2 rb}\sum_{n=0}^{\infty}(2n+1)[a_{1,n}\psi_n(k_{2,1}r)+f_{1,n}\zeta_n(k_{2,1}r)]P_n(\cos\theta);$$

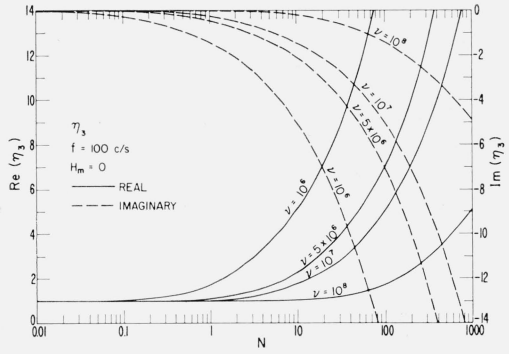

FIGURE 10. *Index of refraction,* $\eta=\mathrm{Re}\eta+\mathrm{iIm}\eta$, *of the model plasma for various electron densities,* N, *and classical collisions,* ν, *in the absence of a superposed magnetic field,* $H_m=0$.

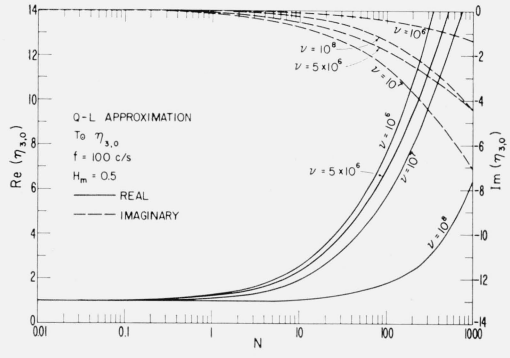

IGURE 11. *Index of refraction,* $\eta_0=\mathrm{Re}\eta_0+\mathrm{iIm}\eta_0$, *of the model plasma for various electron densities,* N, *and classical collisions,* ν *in the presence of a superposed magnetic field,* $H_m=0.5$ *gauss, employing the quasi-longitudinal approximation.*

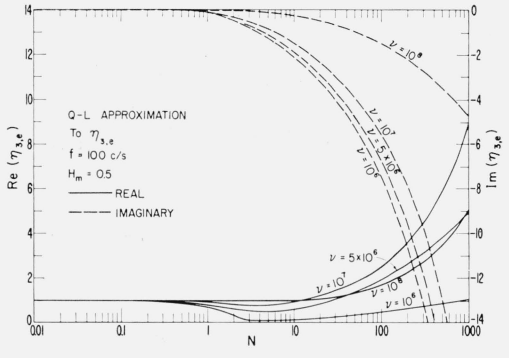

FIGURE 12. *Index of refraction,* $\eta_e=\mathrm{Re}\eta_e+\mathrm{iIm}\eta_e$, *of the model plasma for various electron densities,* N, *and classical collisions,* ν *in the presence of a superposed magnetic field,* $H_m=0.5$ *gauss, employing the quasi-longitudinal approximation.*

the air (k_1) is as before; the mth layer of the ionosphere has wave number $k_{3,m}$, lower edge at $r=c_m$, and Hertz vector,

$$\Pi_{3,m}=\frac{1}{k_{3,m}^2 rb}\sum_{n=0}^{\infty}(2n+1)\left[d_{n,m}\zeta_n(k_{3,m}r)+e_{n,m}\psi_n(k_{3,m}r)\right]P_n(\cos\theta);$$

except for the outermost layer with wave number $k_{3,p}$, which is infinite and thus has only outgoing waves, i.e.,

$$\Pi_{3,p}=\frac{1}{k_{3,p}^2 rb}\sum_{n=0}^{\infty}(2n+1)d_{n,p}\zeta_n(k_{3,p}r)P_n(\cos\theta).$$

In each case, $\Pi_3=\Pi_{3,0}+\Pi_{3,e}$. Similarly, eq (71) can be generalized to take account of coupling at each ionosphere boundary.

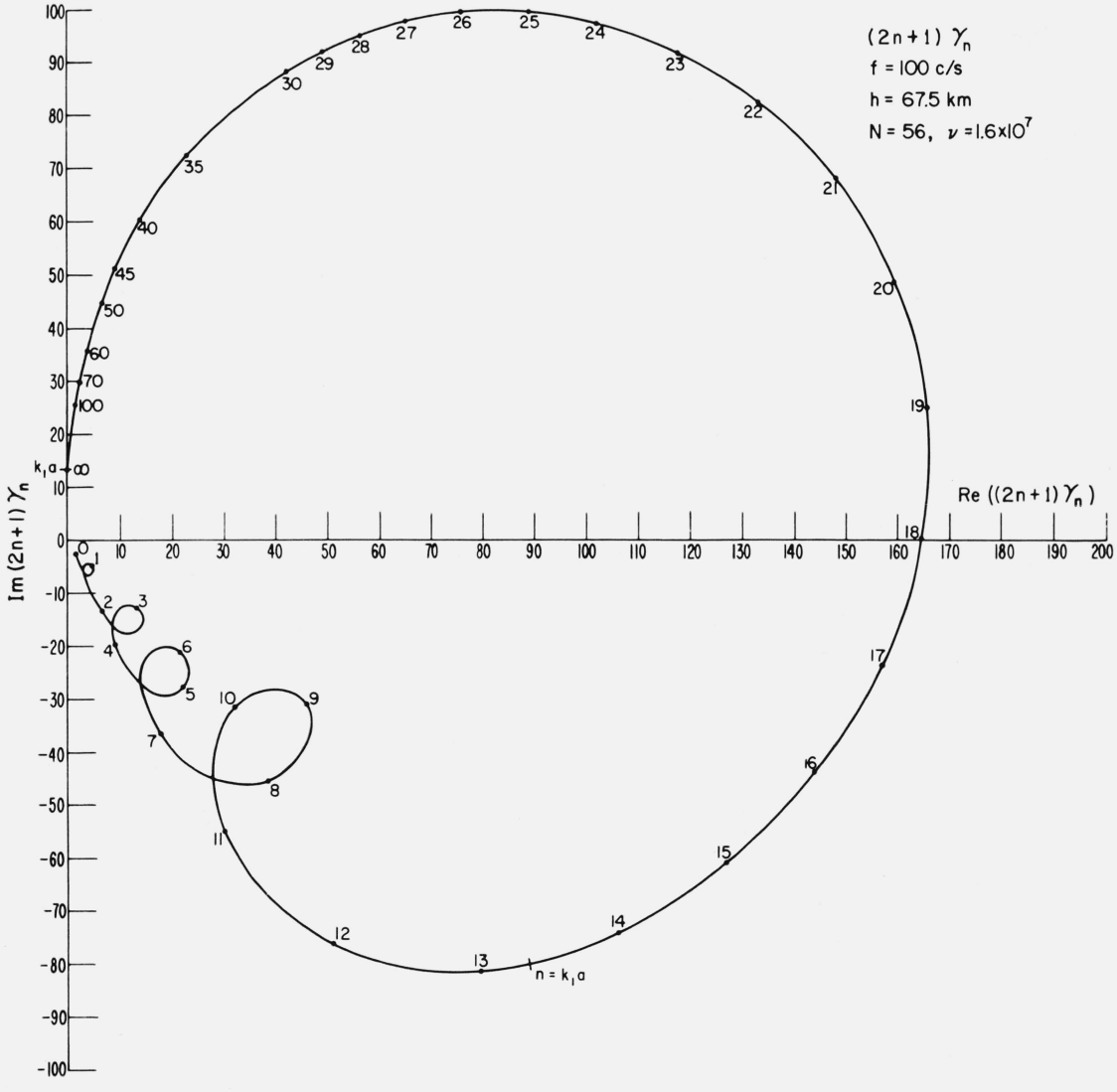

FIGURE 13. *Locus of the coefficient eq (102), of the Legendre function* $P_n(\cos\Theta)$ *for spherical waves of order* n *mapped into the* $(2n+1)\ \gamma_n$*-plane, illustrating both amplitude and phase of the complex spherical wave coefficient.*

2.5. The Watson Transformation

The method proposed by Watson [1919] consisted of forming a complex integral for the Hertz vector, Π,

$$\Pi_1=\frac{1}{k_1^2 rb}\sum_{n=0}^{\infty}(2n+1)P_n(\cos\theta)\frac{b'_n\zeta_n(k_1r)+c'_n\psi_n(k_1r)]}{D_n}, \tag{76}$$

thus,

$$\Pi_1=\frac{i}{k_1^2 rb}\int_C\frac{\nu d\nu}{\cos\nu\pi}P_{\nu-\frac{1}{2}}(-\cos\theta)\frac{[b'_{\nu-\frac{1}{2}}\zeta_{\nu-\frac{1}{2}}k_1r)+c'_{\nu-\frac{1}{2}}\psi_{\nu-\frac{1}{2}}(k_1r)]}{D_{\nu-\frac{1}{2}}} \tag{77}$$

around a suitable contour, C, and taking the sum of the residues at the zeros,

$$D_{\nu-\frac{1}{2}}=0, \tag{78}$$

$$\nu=\nu_s, \tag{79}$$

$$\Pi_1=\frac{-2\pi}{k_1^2 rb}\sum_{s=0}^{\infty}\frac{\nu_s}{\cos\nu_s\pi}\frac{P_{\nu_s-\frac{1}{2}}(-\cos\theta)[b'_{\nu_s-\frac{1}{2}}\zeta_{\nu_s-\frac{1}{2}}(k_1r)+c'_{\nu_s-\frac{1}{2}}\psi_{\nu_s-\frac{1}{2}}(k_1r)]}{\left[\frac{\partial}{\partial\nu}D_{\nu-\frac{1}{2}}\right]_{\nu=\nu_s}}+\int_{-i\infty}^{i\infty}f(\nu)d\nu, \tag{80}$$

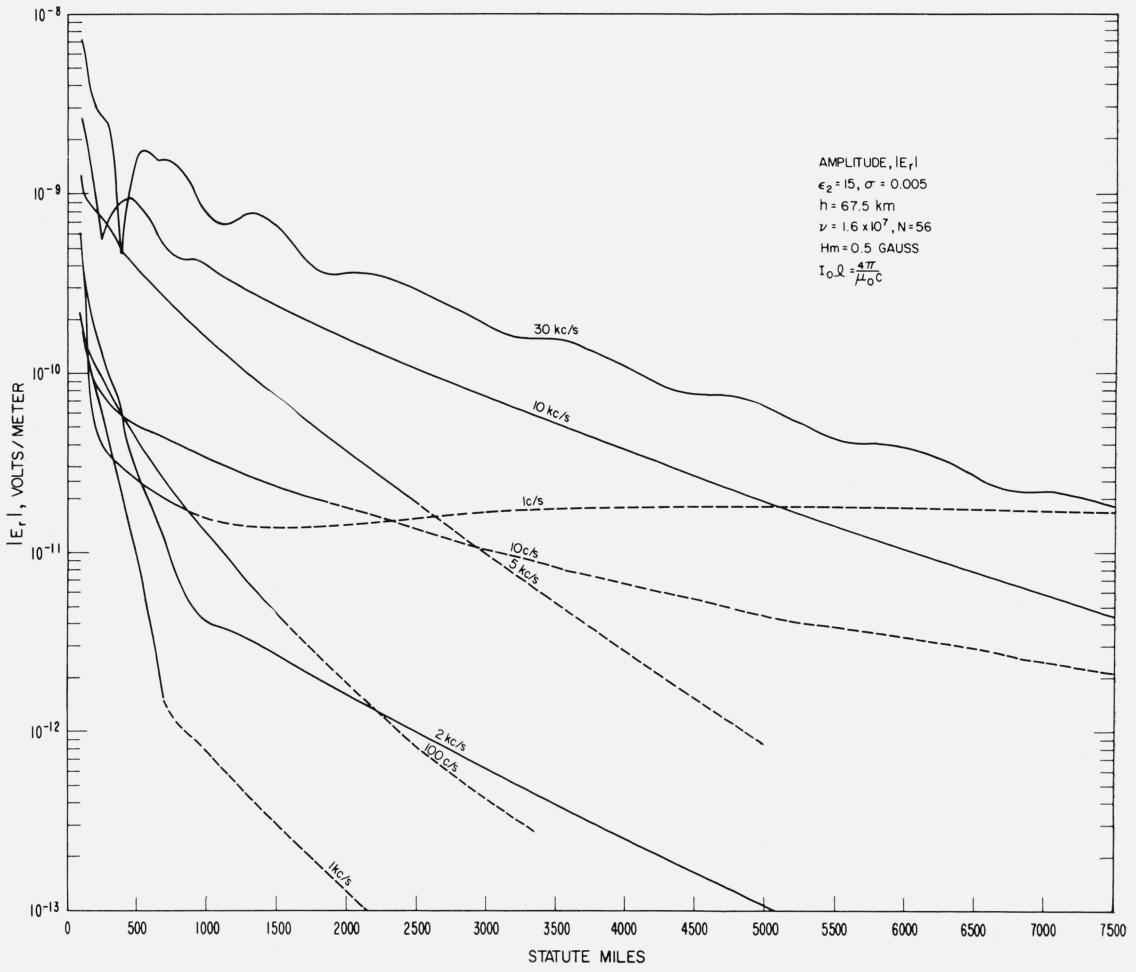

FIGURE 14. *Amplitude of the vertical electric field,* $|E_r|$, *at the surface of the terrestrial sphere* (r=b=a) *excited by a vertical electric time harmonic dipole current source located on the surface of the terrestrial sphere at various frequencies, as a function of distance,* d=aΘ, *on the surface* (r=a) *of the sphere.*

where the line integral along the imaginary axis is usually considered to be negligible, $f(\nu)$ is defined by eq (77), and where

$$b_n=\frac{b_n'}{D_n}, \tag{81}$$

$$c_n=\frac{c_n'}{D_n}, \tag{82}$$

and D_n is the determinant of the matrix eq (73), for example. Whereas the series, $\Pi_1(\nu_s)$, converges rapidly in most practical computations, it would be necessary to evaluate the roots of the eq (78), and form the derivatives of the ζ_ν-waves and ψ_ν-waves with respect to complex order, ν. to maintain the equivalent rigor of the series of zonal harmonics. The exact equivalence of this procedure is of course assured by the theory of functions of the complex variable.

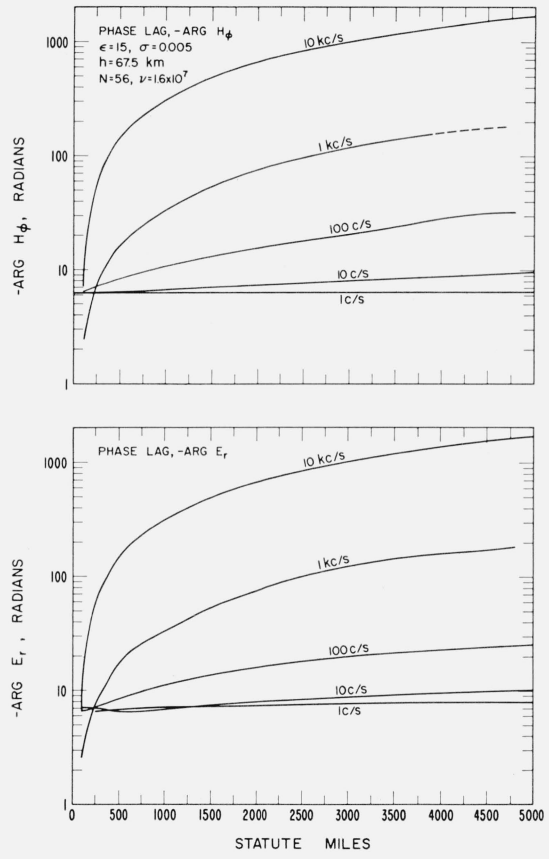

FIGURE 15. *Phase of the vertical electric field,* arg E_r, *and* arg H_ϕ *at the surface of the terrestrial sphere as a function of distance.*

3. Computations

In the particular case, figure 2, of a finitely conducting sphere (without a concentric plasma), the total Hertz vector in the air for the restriction, $r=a$, $b\geq a$,

$$\Pi_{tot}=\Pi_0+\Pi_1, \tag{83}$$

is,

$$\Pi=\frac{-1}{k_1^2ab}\sum_{n=0}^{\infty}(2n+1)\gamma_nP_n(\cos\theta), \tag{84}$$

where,

$$\gamma_n = \frac{\zeta_n(k_1 b)}{\zeta_n'(k_1 a) - \frac{k_1}{k_2}\frac{\psi_n'(k_2 a)}{\psi_n(k_2 a)}\,\zeta_n(k_1 a)}, \tag{85}$$

where the Wronskian identity, [Watson, 1918],

$$\begin{vmatrix} \psi_n & \zeta_n \\ \psi_n' & \zeta_n' \end{vmatrix} = -i, \tag{86}$$

has been employed. From the definitions (62, 63) of $\psi_n(z)$ and $\zeta_n(z)$ and the identity [Watson, 1958],

$$J_\nu'(z) = J_{\nu-1}(z) - \frac{\nu}{z} J_\nu(z), \tag{87}$$

it is easily shown that

$$\psi_n'(z) = \psi_{n-1}(z) - \frac{n}{z}\psi_n(z). \tag{88a}$$

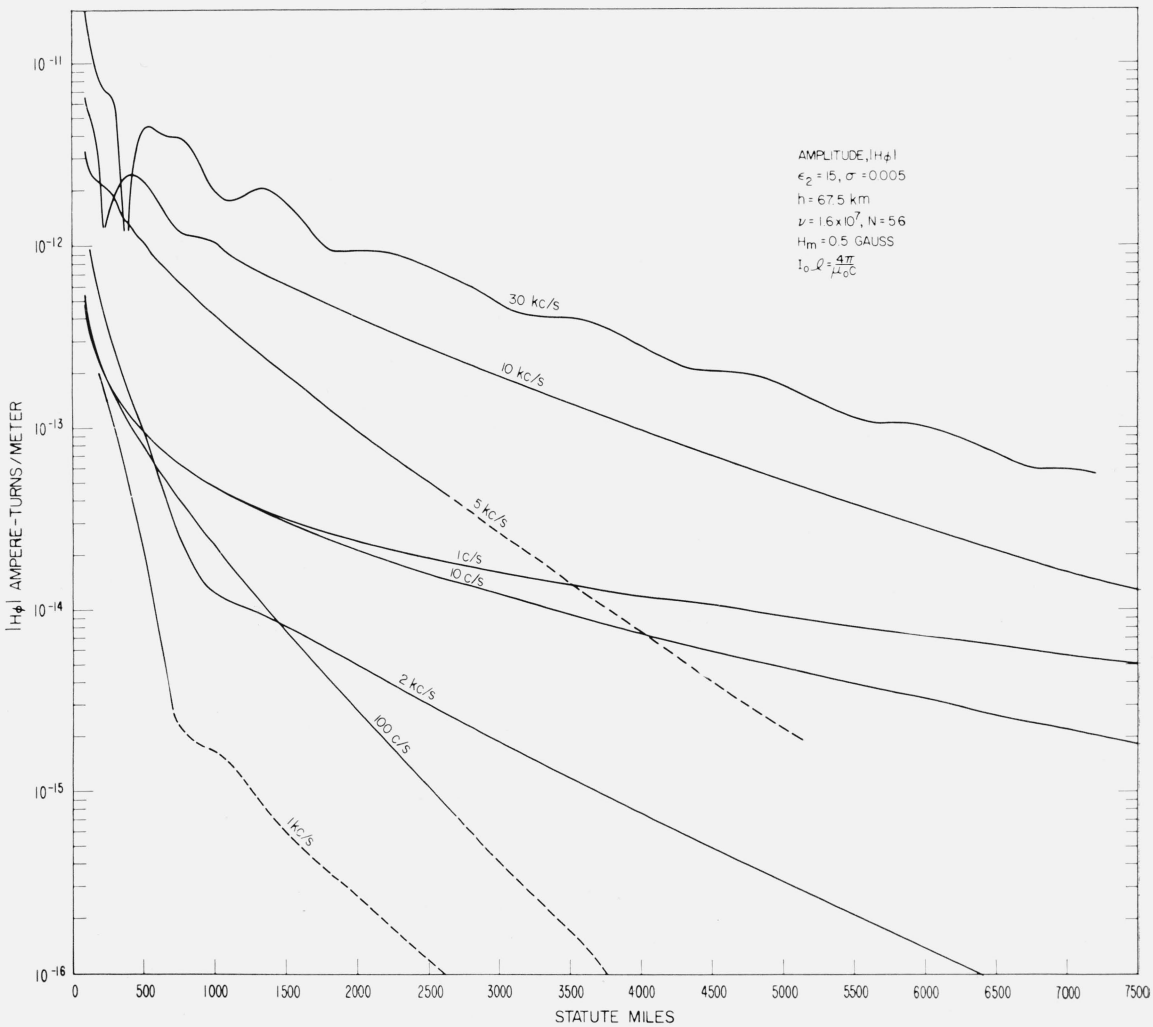

FIGURE 16. *Amplitude of the horizontal magnetic field,* $|H_\phi|$, *at the surface of the terrestrial sphere* (r=b=a) *at various frequencies as a function of distance.*

Similarly,

$$\zeta_n'(z)=\zeta_{n-1}(z)-\frac{n}{z}\,\zeta_n(z). \tag{88b}$$

Thus, γ_n can easily be computed by evaluating the functions $\psi_n(z)$ and $\zeta_n(z)$. Now,

$$\psi_0(z)=\sin z,$$

$$\psi_{-1}(z)=\cos z,$$

and

$$\frac{2n+1}{z}\,\psi_n(z)=\psi_{n+1}(z)+\psi_{n-1}(z). \tag{89}$$

Similarly,

$$\zeta_0(z)=ie^{-iz},$$

$$\zeta_1(z)=-e^{-iz}(1-i/z),$$

and

$$\frac{2n+1}{z}\,\zeta_n(z)=\zeta_{n+1}(z)+\zeta_{n-1}(z). \tag{90}$$

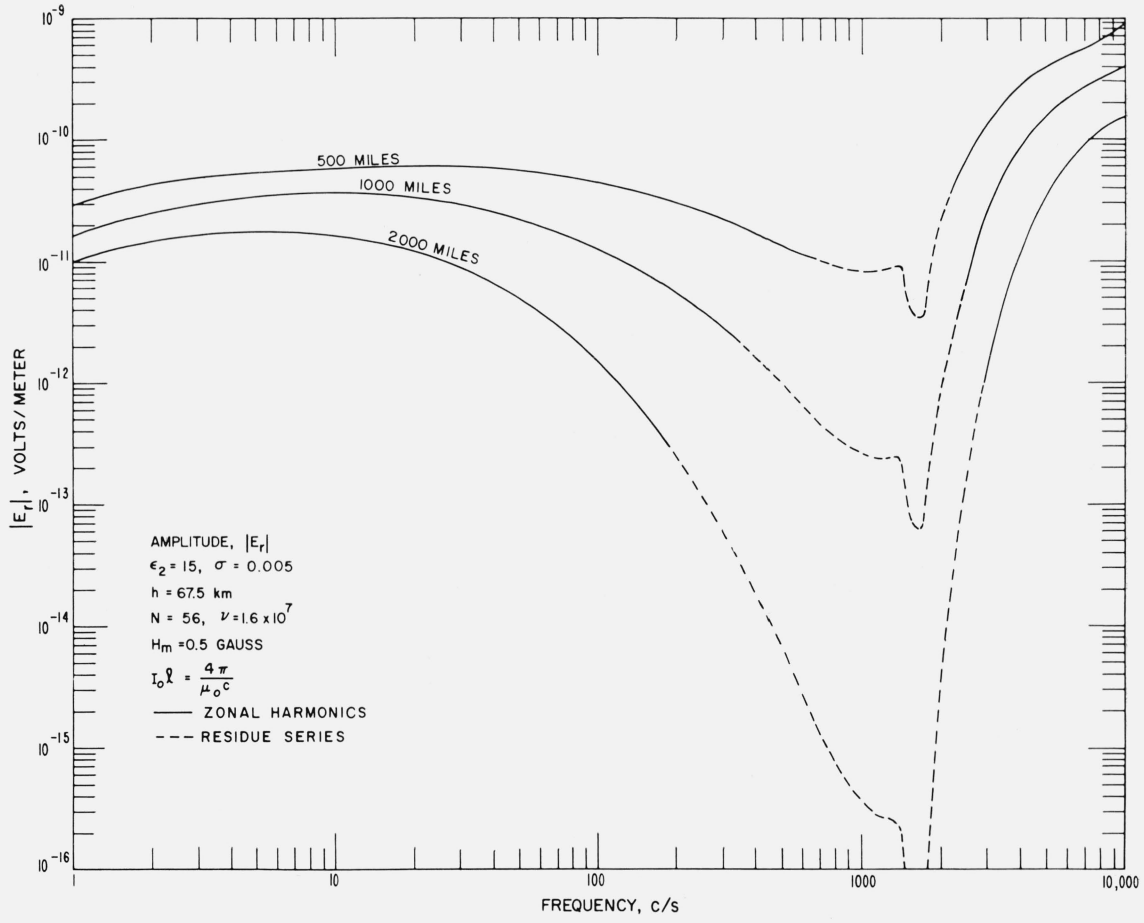

FIGURE 17. *Amplitude of the vertical electric field,* $|E_r|$, *at the surface of the terrestrial sphere* (r=b=a) *excited by a vertical electric time-harmonic dipole current source located on the surface of the terrestrial sphere, as a function of frequency,* f, *at various distances, illustrating an "absorption band" between 300 c/s to 3 kc/s.*

Therefore it would appear that $\psi_n(z)$ and $\zeta_n(z)$ could easily be found for all n. However, for $n > |z|$, eq (89), loses precision with each recursion [Goldstein, and Thaler, 1959], and the series (84) does not converge until $n \gg |k_1 a|$. For $n > |k_1 a|$, the following method of Goldstein and Thaler [1959] is employed:

For $M \gg |z|$, define $F_{M+1}(z)=0$, $F_M(z)=1$, and $F_{n-1}(z)=\frac{2n+1}{z} \times F_n(z) - F_{n+1}(z)$ for $n \leq M$.

Then, with fixed $L>1$, $n \leq (M\text{-}L)$,

$$\psi_n(z)=\alpha F_n(z)+\epsilon(M), \tag{91}$$

where α depends only on z and ϵ can be made arbitrarily small by increasing M. α can be found from

$$\alpha=\frac{\psi_N(z)}{F_N(z)}, \tag{92}$$

for some N for which ψ_n is known, and then $\psi_n(z)$, $N<n<(M\text{-}L)$, can be computed using eq (91).

Since Im $(k_2 a)$ is very large, $\psi_n(k_2 a)$ and $\psi'_n(k_2 a)$ are very large. Therefore, it is more convenient to compute

$$R_n=\frac{\psi'_n(k_2 a)}{\psi_n(k_2 a)}, \tag{93}$$

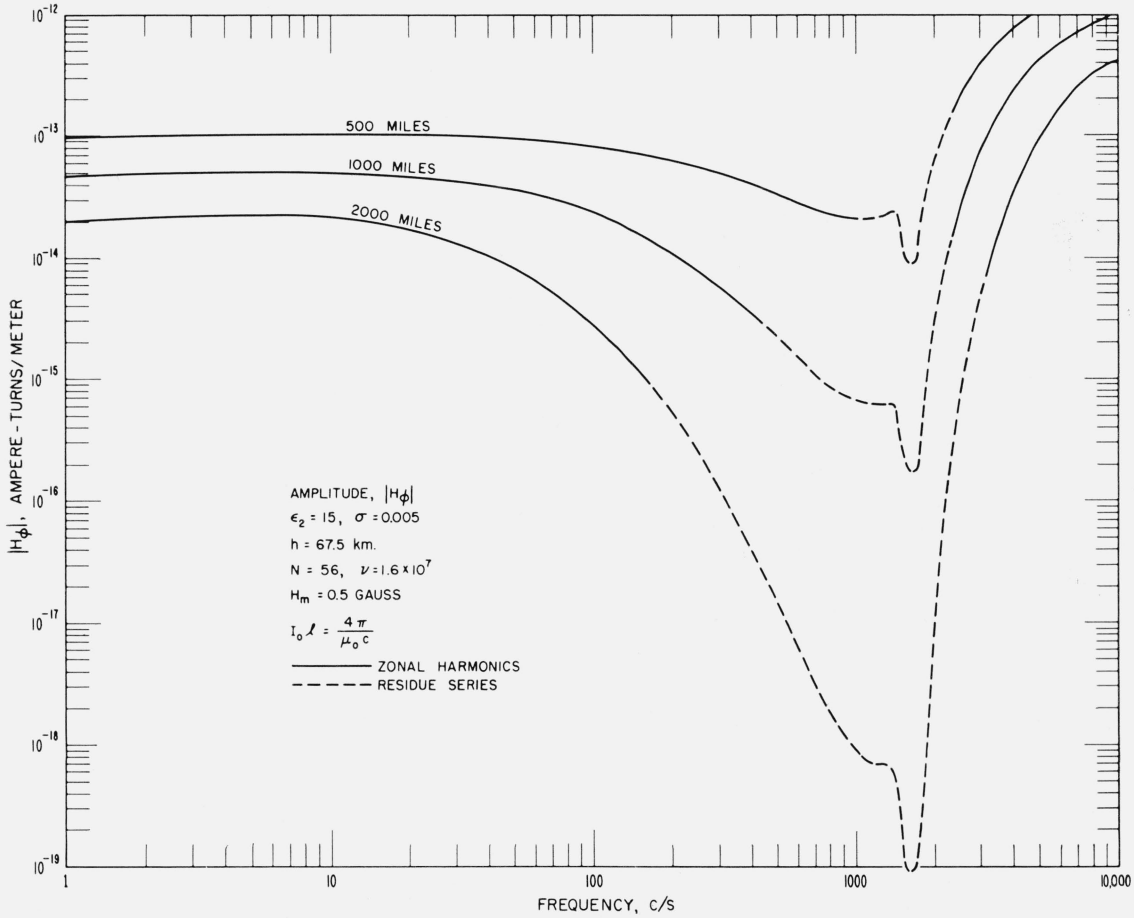

FIGURE 18. *Amplitude of the horizontal magnetic field, $|H_\phi|$ as a function of frequency for various distances, illustrating an "absorption band" between 300 c/s and 3 kc/s.*

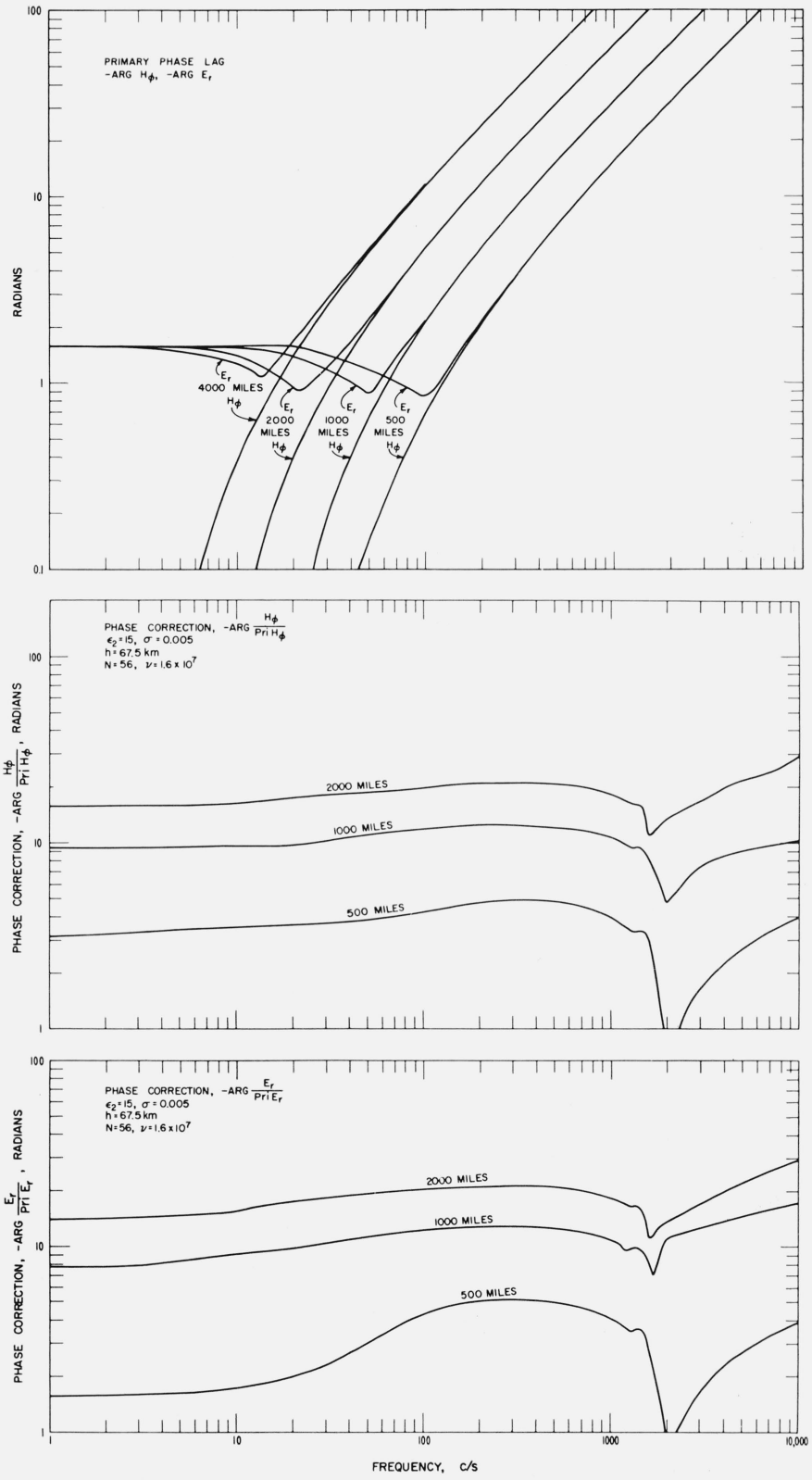

FIGURE 19. *Primary* $-\arg H_\phi, -\arg E_r$ *and secondary phase lag, or phase correction,* $-\arg E_r/E_{r,pri}, -\arg H_\phi/H_{\phi,pri}$, *as a function of frequency.*

$I\delta = \frac{4\pi}{\mu_0 c} \sim 3.34(10^{-2})$

using,

$$R_0=\cot\ (k_2a) \tag{94}$$

and,

$$R_n=\frac{k_2a}{n-k_2aR_{n-1}}-\frac{n}{k_2a} \tag{95}$$

for $n\geq 0$. This recursion formula, which is derived from the well-known recursion formulas for Bessel function [Watson, 1958] will lose precision for $n> |k_2a|$, but for the computations presented in this paper, n remained smaller than $|k_2a|$.

The Legendre polynomials $P_n(x)$ can be computed from the recursion formula [Hobson, 1931],

$$P_{n+1}(x)=\frac{(2n+1)x\,P_n\,(x)-n\,P_{n-1}\,(x)}{n+1},\ (n\geq 1), \tag{96}$$

starting with $P(_0x)=1$ and $P_1(x)=x$.

The convergence of the series (84) is notoriously slow, but the sum can be found from a more quickly convergent series. For $n\gg|k_1a|$ [Watson, 1919],

$$(2n+1)\gamma_n\sim -2k_1a\left(\frac{a}{b}\right)^n. \tag{97}$$

For $l<1$, [Hobson, 1931]

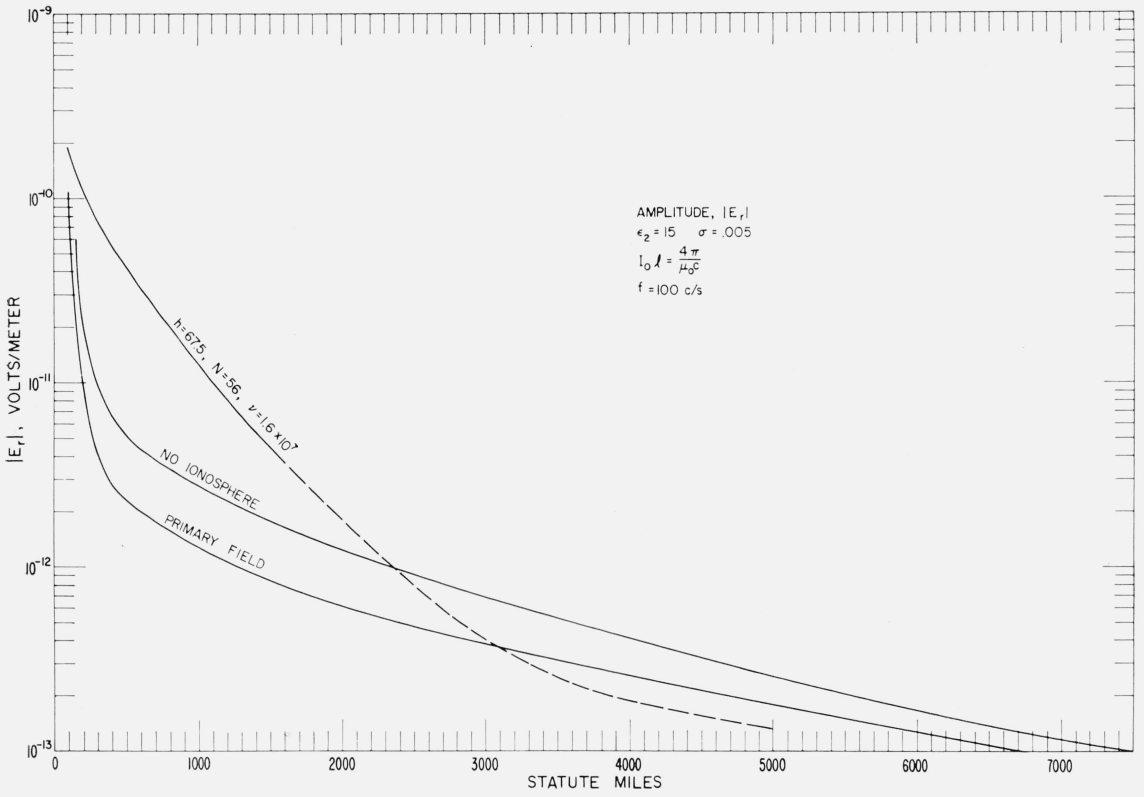

FIGURE 20. *Amplitude of the vertical electric field,* $|E_r|$, *at 100 c/s as a function of distance from the source, illustrating the primary field, the field disturbed by the terrestrial sphere (no ionosphere), and the field disturbed by both the terrestrial sphere and the concentric plasma.*

$I_0l=\frac{4\pi}{\mu_0c}\sim 3.34(10^{-2})$

$$\sum_{n=0}^{\infty} l^n P_n(\cos\theta) = (1 - 1l\cos\theta + l^2)^{-\frac{1}{2}}, \tag{98}$$

so that

$$-\frac{1}{k_1^2 ab}\sum_{n=0}^{\infty} 2k_1 a\left(\frac{a}{b}\right)^n P_n(\cos\theta) = \frac{-2}{k_1 b}\left[1 - 2\left(\frac{a}{b}\right)\cos\theta + \frac{a^2}{b^2}\right]^{-\frac{1}{2}}. \tag{99}$$

Therefore, adding (84) and (99),

$$\Pi_{\text{tot}} = \frac{2}{k_1 b}\left[1 - \frac{2a}{b}\cos\theta + \frac{a^2}{b^2}\right]^{-\frac{1}{2}} - \frac{1}{k_1^2 ab}\sum_{n=0}^{\infty}\left[2k_1 a\left(\frac{a}{b}\right)^n + (2n+1)\gamma_n\right]P_n(\cos\theta). \tag{100}$$

As a result of eq (97),

$$\left[2k_1 a\left(\frac{a}{b}\right)^n + (2n+1)\gamma_n\right] \to 0,$$

as n gets much larger than $k_1 a$, so that the new series (100) converges more quickly than the original series (84). The E_r and H_ϕ fields were computed at a given point, p_0, by computing the Hertz vector Π_{tot} at seven points, p_{-3}, p_{-2}, p_{-1}, p_{-0}, p_1, p_2, p_3, where $p_n = p_0 + n\triangle\theta$ for fixed $\triangle\theta$. The derivatives, eq (5),

$$\frac{\partial\Pi}{\partial\theta}\Big|_{p=p_0}$$

and

$$\frac{\partial^2\Pi}{\partial\theta^2}\Big|_{p=p_0},$$

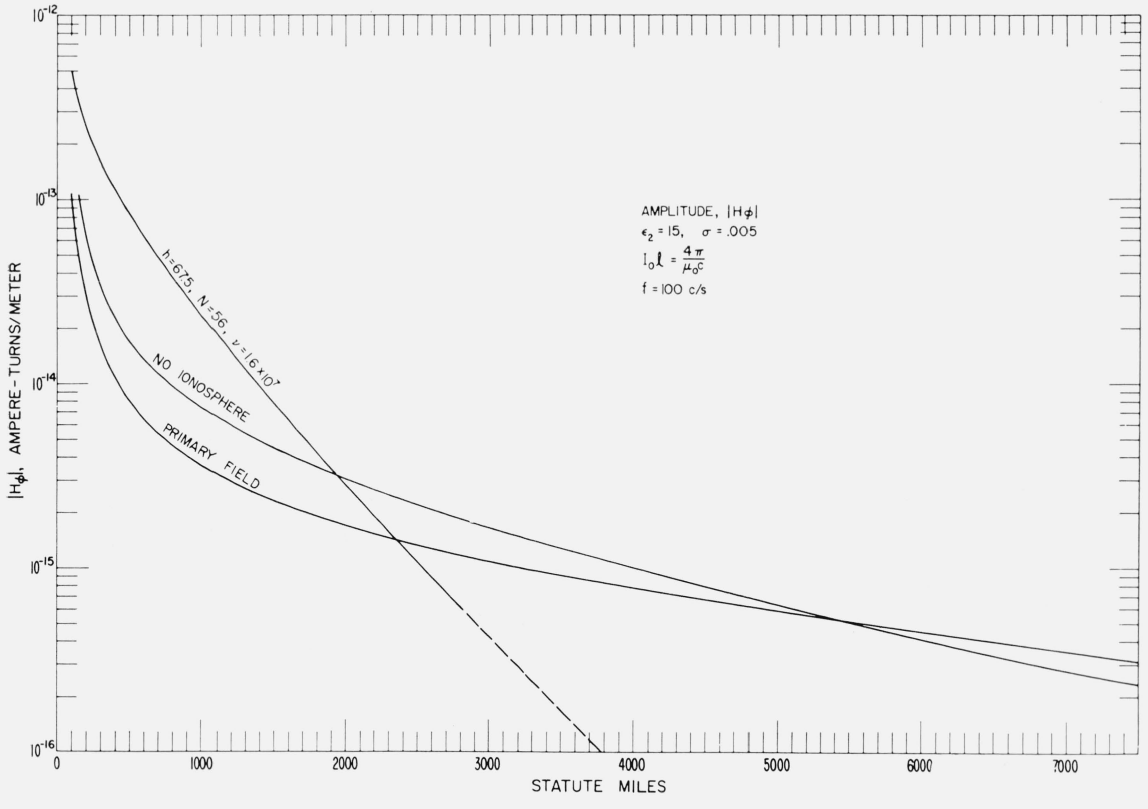

FIGURE 21. *Amplitude of the horizontal magnetic field, $|H_\phi|$, at 100 c/s as a function of distance from the source, illustrating the primary field, the field disturbed by the presence of the terrestrial sphere (no ionosphere), and the field disturbed by both the terrestrial sphere and the concentric plasma.*

$I_0 l = \frac{4\pi}{\mu_0 c} \sim 3.34(10^{-2})$

were then found numerically using the seven point Lagrangian formula [Kopal, 1955]. As a check, the first two derivatives of an orthogonal least-square polynomial fitted to points p_{-2}, $\cdots$, p_2 [Hildebrand, 1956] were computed and compared with the results of the Lagrangian formula. The computed derivatives were then substituted into the appropriate eqs (5) to find the E_r and H_ϕ fields.

For the model, figure 3, which includes the sharply bounded inosphere, computations were made for the case $r=a=b$, the Hertz vector for which can be written with the time function exp ($i\omega t$) suppressed:

$$\Pi_{tot}=\frac{\exp(-ikD)}{-ikD}+\frac{1}{k_1^2a^2b^2}\sum_{n=0}^{\infty}(2n+1)\gamma_nP_n(\cos\theta), \tag{101}$$

where now,

$$\gamma_n=[\zeta_n(k_1a)B_n+\psi_n(k_1a)C_n]D_n^{-1} \tag{102}$$

where

$$B_n=\begin{vmatrix} a_{1,1} & a_{1,0} & a_{1,3} & 0 \\ a_{2,1} & a_{2,0} & a_{2,3} & 0 \\ 0 & a_{3,0} & a_{3,3} & a_{3,4} \\ 0 & a_{4,0} & a_{4,3} & a_{4,4} \end{vmatrix},$$

$$C_n=\begin{vmatrix} a_{1,1} & a_{1,2} & a_{1,0} & 0 \\ a_{2,1} & a_{2,2} & a_{2,0} & 0 \\ 0 & a_{3,2} & a_{3,0} & a_{3,4} \\ 0 & a_{4,2} & a_{4,0} & a_{4,4} \end{vmatrix},$$

and

$$D_n=\begin{vmatrix} a_{1,1} & a_{1,2} & a_{1.3} & 0 \\ a_{2,1} & a_{2,2} & a_{2,3} & 0 \\ 0 & a_{3,2} & a_{3,3} & a_{3,4} \\ 0 & a_{4,2} & a_{4,3} & a_{4,4} \end{vmatrix},$$

for the $a_{i,j}$ defined in (72).

Or, explicitly,

$$\begin{aligned}\gamma_n=&[\phi_n\{[k_2\zeta_n(k_1a)\psi_n'(k_1a)-k_1R_n\zeta_n(k_1a)\psi_n(k_1a)][\zeta_n(k_1a)\psi_n'(k_1c)-\zeta_n'(k_1c)\psi_n(k_1a)]-ik_2\zeta_n'(k_1c)\psi_n(k_1a)\}\\ &-\phi_n'\{[k_1k_2\psi_nk_1a)\zeta_n(k_1c)-k_1^2R_n\psi_n(k_1a)\zeta_n(k_1a)][\zeta_n(k_1a)\psi_n(k_1c)-\zeta_n(k_1c)\psi_n(k_1a)]-ik_2k_1\zeta_n(k_1c)\psi_n(k_1a)\}]\\ &\times[\phi_n\{-k_2[\zeta_n'(k_1a)\psi_n'k_1c)-\psi_n'(k_1a)\zeta_n'(k_1c)]+k_1R_n[\zeta_n(k_1a)\psi_n'(k_1c)-\zeta_n'(k_1c)\psi_n(k_1a)]\}\\ &+\phi_n'\{k_2k_1[\zeta_n'(k_1a)\psi_n(k_1c)-\psi_n'(k_1a)\zeta_n(k_1c)]-k_1^2R_n[\zeta_n(k_1a)\psi_n(k_\perp c)-\zeta_n(k_1c)\psi_n(k_1a)]\}]^{-1},\end{aligned} \tag{103}$$

where,

$$\phi_n=\zeta_n(k_{3,0}c)+\zeta_n(k_{3,e}c),$$

$$\phi_n'=\frac{1}{k_{3,0}}\zeta_n'(k_{3,0}c)+\frac{1}{k_{3,e}}\zeta_n'(k_{3,e}c),$$

and,

$$R_n=\frac{\psi_n'(k_2a)}{\psi_n(k_2a)},$$

as before (93).

The ψ and ζ functions were computed as before, eqs (88–92).

Certain numerical characteristics of the series (101) make possible direct computation of the derivatives using

$$\frac{\partial \Pi}{\partial \theta}=\frac{1}{k_1^2 a^2}\sum_{n=0}^{\infty}(2n+1)\gamma_n \frac{d}{d\theta}P_n(\cos)\,\theta$$

$$=\frac{-\sin\theta}{k_1^2 a^2}\sum_{n=0}^{\infty}(2n+1)\gamma_n P_n'(\cos\theta), \tag{104}$$

where $P_n'(\cos\theta)$ denotes $\dfrac{d}{d(\cos\theta)}P_n(\cos\theta)$.

Similarly,

$$\frac{\partial^2 \Pi}{\partial \theta^2}=\frac{1}{k_1^2 a^2}\sum_{n=0}^{\infty}(2n+1)\gamma_n[\sin^2\theta P_n''(\cos\theta)-\cos\theta P_n'(\cos\theta)]$$

$$=\frac{\sin^2\theta}{k_1^2 a^2}\sum_{n=0}^{\infty}(2n+1)\gamma_n P_n''(\cos\theta)+\frac{\cos\theta}{\sin\theta}\frac{\partial \Pi}{\partial \theta}. \tag{105}$$

The derivatives of $P_n(x)$ can be found from eq (96),

$$P_{n+1}'(x)=P_{n-1}'(x)+(2n+1)P_n(x), \tag{106}$$

and [Hobson, 1931]

$$P_{n+1}''(x)=P_{n-1}''(x)+(2n+1)P_n'(x). \tag{107}$$

The series, eqs (104, 105), converge even more slowly than the original series, eq (101). However, for $n>>|k_1 a|$, $(2n+1)\gamma_n \sim ik_1 a$, so, as before, the series can be transformed to improve convergence using [Hobson, 1931]

$$\sum_{n=m}^{\infty} h^n \frac{d^m P_n(\cos\theta)}{d(\cos\theta)^m}=\frac{1.3.\cdots(2m-1)h^m}{(1-2h\cos\theta+h^2)^{m+\frac{1}{2}}}, \qquad (h<1) \tag{108}$$

Substitution of the derivatives into eq (5) yields the E_r and H_ϕ fields.

The number of terms required for graphical accuracy in $|E_r|$ varied from about 700 at 10 c/s to about 3,000 at 10 kc/s. The CDC–1604 computer could compute about 830 γ_n, eq (102), per minute. Using these stored γ_n, the fields could be found for 40 different values of θ (distances) per minute per 1,000 terms required.

At frequencies less than about 1,000 c/s, if low electron densities (<100 electrons/cm)^2 are assumed, precision is lost during summation of series (105). This loss of precision increases with increasing θ, and limits the usefulness of the zonal harmonics technique at ELF.

4. Discussion

A series of computations was carried out based on the model of a terrestrial sphere with a vertical electric dipole source current moment, eq (7), $I_0 l=\dfrac{4\pi}{\mu_0 c}$, on the surface of the sphere.[4] The field at the surface of the sphere, $r=a$, figure 2, was described by the computation. Such a field is the exact equivalent of the ground wave described by van der Pol and Bremmer [1937, 1938, 1949] for example, utilizing the Watson transformation (section 2.5). Whereas, the works of van der Pol and Bremmer [1937, 1938, 1949] employ a long series of approximations

[4] $I_0 l=\dfrac{4\pi}{\mu_0 c}\sim 3.34(10^{-2})$ amp—m. This is equivalent to the conventional notion of radiated power, P_r, as follows [Johler, 1961]: $P_r=1.6(10^{-3})\omega^2 (I_0 l)^2/Z_0$, where $Z_0\sim 120\pi$ (impedance of space). Such a radiation field cannot very readily be measured at ELF/VLF since the induction and electrostatic fields are not negligible.

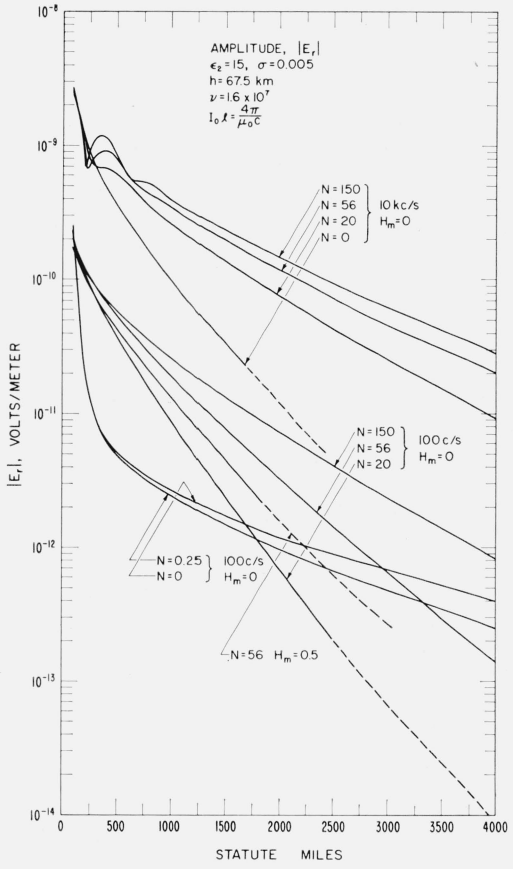

FIGURE 22. *Amplitude of the vertical electric field,* $|E_r|$, *as a function of distance for the terrestrial sphere with various model concentric plasmas at 10 kc/s,* ($H_m=0$, $N=0$, 20, 56, 150) *and 100 c/s* ($H_m=0$, 0.5, $N=0$, 0.25, 20, 56, 150) *illustrating the effect of the earth's magnetic field and different electron densities.*

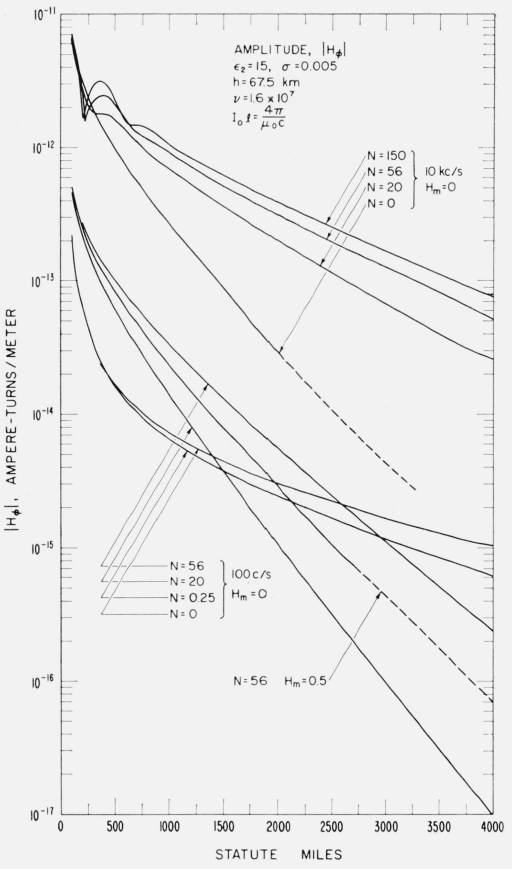

FIGURE 23. *Amplitude of the horizontal magnetic field,* $|H_\phi|$, *as a function of distance for the terrestrial sphere with various model concentric plasmas at 10 kc/s,* ($H_m=0$, $N=0$, 20, 56, 150) *and 100 c/s* ($H_m=0$, 0.5, $N=0$, 0.25, 20, 56, 150) *illustrating the effect of the earth's magnetic field and different electron densities.*

to achieve numerical mastery of the very difficult formulas resulting from the Watson transformation, this solution does not employ any approximations, leaving only the assumed model. This solution is also equivalent to the "acoustical shadow of a sphere" described by Lord Rayleigh [1904], and indeed some of the curves show a close resemblance. Rayleigh, however, did not treat the field at the surface of the sphere but at considerable distance.

The regular decrement of the amplitude of the ground wave as a function of distance can be noted, figures 6 and 8, for both the $|E_r|$ field and the $|H_\phi|$ field, at frequencies of 1, 10, 100, 1000 c/s. However, near the antipode of the transmitter, $d=10{,}000$ to 12,500 statute miles, an interference pattern or standing wave can be noted as a result of the wave traveling around the earth in the opposite $(-\theta)$ direction. The corresponding phase curves, arg E_r, arg H_ϕ, are illustrated, figures 7 and 9. Whereas, the conductivity and dielectric constant are assumed to be finite, ($\epsilon_2=15$, $\sigma=0.005$ mhos/meter), the second term in the denominator of eq (78),

$$\left|\frac{k_1}{k_2}\frac{\psi_n'(k_2a)}{\psi_n(k_2a)}\,\zeta_n(k_1a)\right| << \left|\zeta_n'(k_1a)\right|,$$

is quite small compared with the first term (of the order of 10^4 less) at 1 c/s and 10 c/s. The conductivity terms become significant at the frequencies greater than approximately 500 c/s.

The introduction of a concentric plasma, figures 3 and 4, is quite intricate. However, to gain some insight into the propagation of waves at great wavelengths, and demonstrate

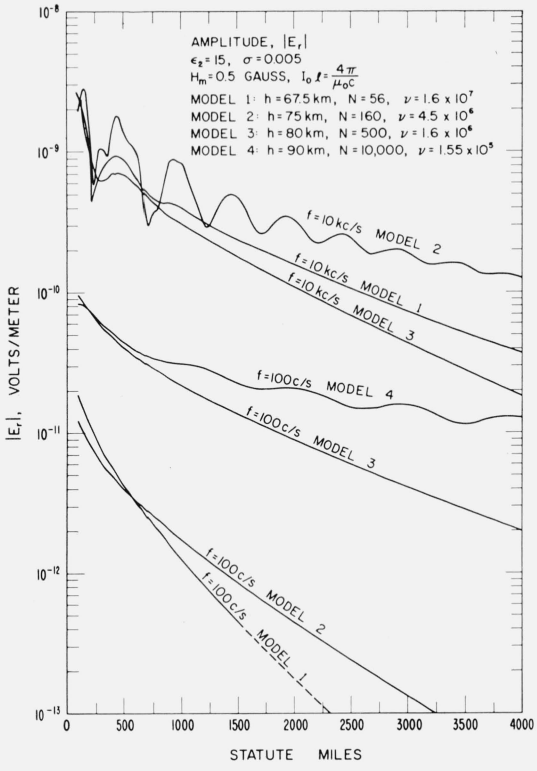

FIGURE 24. *Amplitude of the vertical electric,* $|E_r|$, *field as a function of distance, illustrating various reflection heights,* h, *of the concentric plasma,* c=a+h, *and corresponding typical "daytime-noon" model plasmas (electron densities,* N, *and collision frequencies,* ν).

$I_0 l = \frac{4\pi}{\mu_0 c} \sim 3.34(10^{-2})$

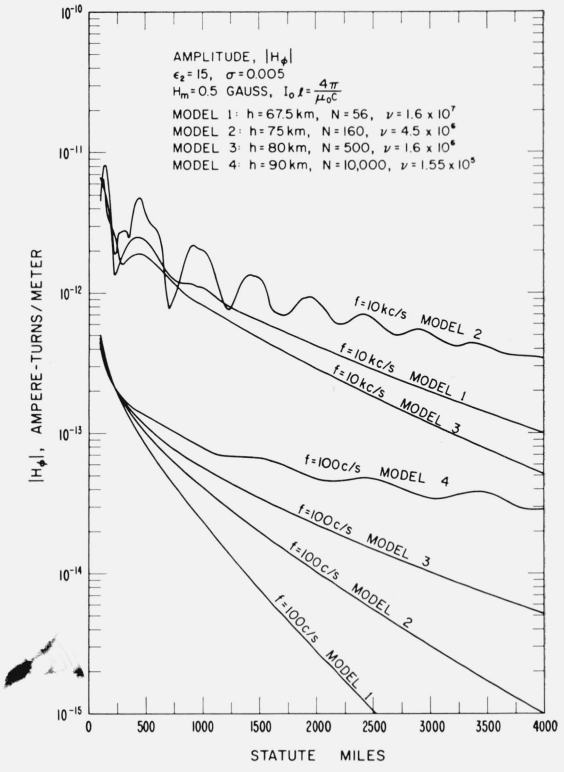

FIGURE 25. *Amplitude of the horizontal magnetic,* $|H_\phi|$, *field as a function of distance, illustrating various reflection heights,* h, *of the concentric plasma,* c=a+h, *and corresponding typical "daytime-noon" model plasmas (electron densities,* N, *and collision frequencies,* ν).

$I_0 = \frac{4\pi}{\mu_0 c} \sim 3.34(10^{-2})$

the computational value of zonal harmonics, the particular case, figure 3, of a terrestrial sphere of finite conductivity surrounded by a concentric plasma was evaluated for the special situation in which transmitter and receiver were located on the surface of the sphere, $h_1=h_2=0$, as was illustrated for the ground wave case. The index of refraction of the concentric plasma was calculated, neglecting the earth's magnetic fields, $H_m=0$, figure 10, and introducing the earth's magnetic field, $H_m=0.5$ gauss with the aid of the Q–L approximation, figures 11 and 12, for various collision frequencies, ν, and electron densities, N(electrons/cm^2). Figure 13 illustrates the behavior of the complex coefficient $(2n+1)\,\gamma_n$, eq (102), of the Legendre polynomial $P_n(\cos\theta)$. Typically, the "loops" in the path occur for $n<k_1a$, the important terms are those for $k_1a \leqq n < 2k_1a$, and $(2n+1)\,\gamma_n$ approaches ik_1a as n approaches infinity.

The introduction of the concentric plasma causes a drastic change in the detail of the propagated field, figures 14 and 16. The space between the concentric plasma and the terrestrial sphere, k_1, figure 3, is now filled with waves trapped by the two boundaries, $r=a$, $r=c$. Thus, figure 5, there are upgoing spherical waves, ζ-waves, and downgoing spherical waves, ψ-waves, whereas in the medium above the outer boundary, $r \geqq c$, there are only upgoing, ζ_0-waves and ζ_e-waves (ordinary and extraordinary), and in the medium below the inner boundary there are only ingoing ψ-waves. These spherical waves traveling in the radial direction, upon summation, build up in the medium between $r=a$ and $r=c$ waves traveling the direction $(\pm\theta)$ of increased angular distance.

The regular nature of the field curves, $|E_r|$ and $|H_\phi|$, as a function of distance, d, figures 14 and 16, indicates a single wave propagated in the θ-direction around the terrestrial sphere in the medium k_1. Near the antipode of the transmitter, however, waves traveling in opposite

directions can be noted as a standing wave, with a half wavelength between minima, as was noted in the case of the ground wave. At the lower frequencies, 100 c/s, and higher conducting concentric model plasmas, figures 24 and 25, this phenomenon can be noted at short distances ($<$4,000 statute miles). Similar standing wave phenomena can be noted at the higher frequencies, 10 kc/s, figures 24 and 25, and 30 kc/s, figures 14 and 16, for intermediate conductivity concentric model plasma, indicating interaction between two or more waves. The distance between minima are in this case much greater than a wavelength, and seem to damp out with distance.

The variation in the amplitude, $|E_r|$, $|H_\phi|$, figures 17 and 18 and the phase, figure 19, as a function of frequency is illustrated. These curves illustrate the spectrum mutilation [Johler, 1962] of the pulses propagated through the media defined by this paper. It is interesting to note an "absorption band," between frequencies 300 c/s and 3,000 c/s, for the assumed model, figures 17 and 18. This absorption band is also reflected in the phase correction curves, figure 19. The primary field phase is also illustrated. It should be noted that phase is presented as a lag, $-\arg E_r$, $-\arg H_\phi$, or $-\arg E_r/E_{r,\,pri}$, $-\arg H_\phi/H_{\phi,\,pri}$, where $E_{r,\,pri}$ and $H_{\phi,\,pri}$ refer to the primary fields.

A comparison (at 100 c/s) of the primary field, the ground wave (no ionosphere), and the field with the concentric plasma (ionosphere) is illustrated for the E_r-field, figure 20, and the H_ϕ-field, figure 21. For the assumed model, the attenuation *rate* of the field increases successively as the terrestrial sphere and the concentric plasma are introduced.

It is evident, figures 22 and 23, that the electron density, N, is the most important concentric plasma (ionosphere) factor governing the field. The intensity of the superposed magnetic field (earth's magnetic field) is only secondary. It should be noted, figures 22 and 23, that the field reduces to the ground wave for $N=0$. The vertical electric field $|E_r|$ and the horizontal magnetic field $|H_\phi|$ are illustrated. Model ionospheres employed in other analyses [Johler and Harper, 1962] by selecting the electron concentration values of the earth's ionosphere at daytime noon, together with appropriate collision frequencies, are illustrated, figures 24 and 25. It is interesting to note the increase in the field at 100 c/s as the higher conductivity models are successively employed (model 1, 2, 3, 4). However, an intermediate model 2 exhibits not only the greater field at 10 kc/s but also the standing wave with distances between minima much greater than a wavelength.

Since, analysis is designed to gain some insight into the very complicated behavior of terrestrial radio waves near the earth, and also to demonstrate the technique of zonal harmonics as applied to the radio problem employing modern techniques of computation, considerable caution must be exercised in the interpretation of results from a practical viewpoint. The roughness, daytime-nighttime changes, the temporal variations and the multiplicity of frequencies in a radio signal, and coupling at the ionosphere all could tend to mask the theoretical phenomena described. Furthermore, it would be desirable to investigate the effect of the heavy ions numerically. But the detailed investigation of these matters is reserved for future studies.

5. Conclusions

The results of this paper demonstrate that the field of the low frequency or long wavelength radio wave, less than approximately 50 kc/s, can indeed by evaluated by a summation of a series of zonal harmonics. Whereas the number of terms in the series could become quite large, the speed with which these terms can be summed on a large scale computer offsets the complications introduced by the Watson transformation.

The detailed structure of the field is characterized in the absence of a concentric plasma (no ionosphere) by the quite regular behavior of the ground wave as a function of distance. Indeed, the steady decrement of the ground wave field is modified only near the antipode, whereupon an interference pattern or standing wave as a function of distance is noted as a result of interference between waves traveling "around the world" in opposite directions from the transmitter.

The introduction of the concentric electron-ion plasma shell traps the waves leaking into space, which upon reflection from the plasma build up traveling waves in the direction of increased distance from the transmitter. Thus, the series of zonal harmonics comprises individual waves which are traveling in the radial direction with respect to the center of the sphere and standing in the direction of increased angular distance around the sphere. These waves when summed build up the wave progressing in the direction of increased angular distance. But under certain special conditions such spherical waves also build up a standing wave in the same direction which can be interpreted as a multiplicity of traveling waves such as two waves traveling in opposite directions at the antipode of the transmitter.

The results of the computations indicate that full rigor can be achieved with comparative ease at frequencies less than 50 kc/s, leaving only the assumed model for the transmitter and the propagation medium and avoiding the complications of the Watson transformation.

The results of this paper suggest refinements of the computations, such as the introduction of terrestrial sphere stratification, continuous ionosphere stratification, polarization coupling at the ionosphere, and the effect of heavy ions.

6. References

Booker, H. G., The propagation of wave packets incident obliquely on a stratified doubly refracting ionosphere, Phil. Trans. **A237,** 411, (1939).

Bremmer, H., Terrestrial radio waves; theory of propagation (Elsevier Publ. Co., New York, N.Y., 1949).

Budden, K. G., The reflection of very low frequency radio waves at the surface of a sharply bounded ionosphere with superimposed magnetic field, Phil. Mag. **42,** No. 2, 833 (1951).

Campbell, W. H., Natural electromagnetic energy below the ELF range, J. Research NBS **64D** (Radio Prop.), No. 4, 409 (July-Aug. 1960).

Debye, P., Der Lichtdruck auf Kugeln von beliebigem Material, Ann. Physik (Leipzig) **XXX** (**30**), 57–136 (1909).

Goldstein, M., and R. M. Thaler, Recurrence techniques for the calculation of Bessel functions, MTAC **XIII** (**13**), 102–108 (1959).

Hertz, H., Die Kräfte electrischer Schwingungen behandelt nach der Maxwell' schen Theorie, Ann. Physik und Chemie, Neue Folge **XXXVI** (**36**), 1, Leipzig (1889).

Hildebrand, F. B., Introduction to Numerical Analysis (McGraw-Hill Book Co., Inc., New York, 1956).

Hobson, E. W., The theory of spherical and ellipsoidal harmonics (The University Press, Cambridge, England, 1931).

Jahnke, E., and F. Emde, Tables of Functions, 4th ed. (Dover Publications, New York, 1945).

Jean, A. G., A. C. Murphy, J. R. Wait, and D. F. Wasmundt, Observed attenuation rate of ELF radio waves, J. Research NBS **65D** (Radio Prop.), No. 5, 475–479 (Sept.–Oct. 1961).

Johler, J. R., Magneto-ionic propagation phenomena in low- and very low-radiofrequency waves reflected by the ionosphere, J. Research NBS **65D** (Radio Prop.), No. 1, 53–65 (Jan.–Feb. 1961).

Johler, J. R., On the analysis of LF ionospheric phenomena, J. Research NBS **65D** (Radio Prop.), No. 5, 507 (Sept.–Oct. 1961).

Johler, J. R., and J. D. Harper, Jr., Reflection and transmission of radio waves at a continuously stratified plasma with arbitrary magnetic induction, J. Research NBS **66D** (Radio Prop.), No. 1, 81 (Jan.–Feb. 1962).

Johler, J. R., and L. C. Walters, On the theory of reflection of low- and very low-radiofrequency waves from the ionosphere, J. Research NBS **64D**, No. 3, 269–285 (May–June 1960).

Johler, J. R., L. C. Walters, and J. D. Harper, Jr., Low- and very low-radiofrequency model ionosphere reflection coefficients, NBS Tech. Note 69, PB161570, U.S. Dept. of Commerce, Office of Technical Services, Washington 25, D.C. (July 1, 1960).

Kopal, Z., Numerical Analysis (John Wiley & Sons, Inc., New York, 1955).

Love, A. E. H., The transmission of electric waves over the surface of the earth, Phil. Trans. **A215,** 105–141 (1915).

Macdonald, H. M., The bending of electric waves round a conducting obstacle, Pts. I, II, III, IV, Proc. Roy. Soc. **71,** 251 (1903); Proc. Roy. Soc. **72,** 59 (1904); Roy. Soc. Phil. Trans. **A210,** 113 (1911); Proc. Roy. Soc. **90,** 50–61, (1914).

March, H. W., Über die Ausbreitung der Wellen der drahtlosen Telegraphie auf der Erdkugel, Ann. Physik, Vierte Folge **XXXVII** (**37**), 29–50 (1912).

Nicholson, J. W., On the bending of electric waves round a large sphere, Pts. I, II, III, IV, Phil. Mag., Ser. 6, **19,** 516 (1910); **20,** 157 (1910); **21,** 62, 281 (1911); **19,** 757 (1910).

648645—62——9

Pfister, W., Studies of the refractive index in the ionosphere: the effects of the collision frequency and of ions, Phil. Soc. London, Physics of the Ionosphere (1955).
Phelps, A. V., Propagation constants for electromagnetic waves in weakly ionized, dry air, J. Appl. Phys. **21,** No. 10, 1723–1729 (October 1960).
Pierce, E. T., Some ELF Phenomena, J. Research NBS **64D** (Radio Prop.), No. 4, 383 (July–Aug. 1960).
Poincaré, H., Sur la diffraction des ondes electriques: à propos d' un article de M. Macdonald, Proc. Roy. Soc. London **A72,** 42–52 (1904).
Poincaré, H., Sur la diffraction des ondes hertgiennes, Rend. Circ. Mat., Palermo, t. 29, p. 169 (1910).
Ratcliffe, J. A., The magneto-ionic theory and its applications to the ionosphere (Cambridge Univ. Press, England, 1959).
Rayleigh, Lord, On the acoustic shadow of a sphere, with appendix giving the values of Legendre's functions from P_0 to P_{20} at intervals of 5 degrees by Prof. A. Lodge, Phil. Trans. Roy. Soc., London **A203,** 87–110 (1904).
Stratton, J. A., Electromagnetic Theory (McGraw-Hill Book Co., Inc., New York, N. Y., 1941).
van der Pol, Balth, and H. Bremmer, The diffraction of electromagnetic waves from an electrical point source round a finitely conducting sphere, with applications to radiotelegraphy and the theory of the rainbow, Phil. Mag. [7] **24,** Pt. I, 141 (July 1937); pt. II, 825 (Nov. 1937); Supp. J. Science **25,** 817 (June 1938).
von Rybczyński, W., Über die Ausbreitung der Wellen der drahtlosen Telegraphie auf der Erdkugel, Ann. Physik, Vierte Folge, **XLI** (**41**), 191–208 (Leipzig, 1913).
Wait, J. R., The mode theory of VLF ionospheric propagation for finite ground conductivity, Proc. I.R.E. **45,** 760 (1957).
Wait, J. R., Terrestrial propagation of VLF radio waves, J. Research NBS **64D** (Radio Prop.), No. 2, 153–204 (Mar.–Apr. 1960).
Wait, J. R., Mode theory and propagation of ELF radio waves, J. Research NBS **64D** (Radio Prop.), No. 4, 387, (July–Aug. 1960.)
Wait, J. R., E. M. radiation, from cylindrical structures, (Pergammon Press, 1959).
Watson, G. N., The diffraction of electric waves by the earth, Proc. Roy. Soc. London **AXCV (95),** 83 (1918).
Watson, G. N., The transmission of electric waves round the earth, Proc. Roy. Soc. London **ACXV (95),** 546 (1919).
Watson, G. N., Bessel functions, 2d edition (Cambridge Univ. Press, London, 1958.

7. Appendix

The coefficients of the quartic (23) are:

$$a_0=(a^2-1)^2\left\{1-\frac{s}{s^2-h^2}\right\}+(a^2-1)\left\{\frac{1}{s}+\frac{s-2}{s^2-h^2}+\frac{a_L{}^2h_T{}^2}{s(s^2-h^2)}\right\}+\frac{s-1}{s(s^2-h^2)},$$

$$a_1=2\,\frac{h_Lh_Ta_L}{s(s^2-h^2)}\,(a^2-1)\,,$$

$$a_2=\left\{2\left[1-\frac{s}{s^2-h^2}\right]+\frac{h_L{}^2}{s(s^2-h^2)}\right\}\,(a^2-1)\,,$$

$$a_3=2\,\frac{h_Lh_Ta_L}{s(s^2-h^2)}=-a_1\sec^2\phi_i\,,$$

$$a_4=1-\frac{s^2-h_L{}^2}{s(s^2-h_2)},$$

where,

$$s=\frac{\omega^2}{\omega_N^2}\left[1-i\,\frac{\nu}{\omega}\right], \qquad h=\frac{\omega_H\omega}{\omega_n^2},$$

$$h_L=-h\sin I, \qquad a=\sin\phi_1,$$

$$h_T=h\cos I, \qquad \omega_N^2=Ne^2/\kappa m,$$

$$a_L = \sin\phi_i \cos\phi_a, \qquad \omega_H = \mu_0 e H_m / m,$$

$$a_T = \sin\phi_i \sin\phi_a, \qquad \kappa = 1/c^2\mu_0 = \epsilon_0.$$

These coefficients can be modified for electron-ion collisions proportional to energy [Johler and Harper, 1962]. The angle of incidence, eq (47), $\phi_i = \sin^{-1}\left[\frac{Er}{E\theta}\right]$, can be found for each elementary spherical wave, thus, the ζ_n-wave can be written for two wave types, 1, 2,

$$\left[\frac{E_{\theta,n}}{E_{r,n}}\right]_{1,2} = \left[\frac{k_i r}{n(n+1)}(-\sin\theta)\frac{\left\{P'_n(\cos\theta) \pm \frac{2}{\pi i} Q'_n(\cos\theta)\right\}\zeta'_n(k_1 r)}{\left\{P_n(\cos\theta) \pm \frac{2}{\pi i} Q_n(\cos\theta)\right\}\zeta_n(k^1 r)}\right]_{r=c} \sim \sqrt{\frac{k_1^2 c^2}{n^2} - 1}$$

and the ψ_n-wave,

$$\left[\frac{E_{\theta,n}}{E_{r,n}}\right]_{1,2} = \left[\frac{k_1 r}{n(n+1)}(-\sin\theta)\frac{\left\{P'_n(\cos\theta) \pm \frac{2}{\pi i} Q'_n(\cos\theta)\right\}\psi'_n(k_1 r)}{\left\{P_n(\cos\theta) \pm \frac{2}{\pi i} Q_n(\cos\theta)\right\}\psi_n(k_1 r)}\right]_{r=c} \sim \sqrt{\frac{k_1^2 c^2}{n^2} - 1}$$

and

$$\phi_i = \sin^{-1} - \zeta \frac{E_r}{E\theta}$$

a complex angle of incidence, or,

$$\sin^2\phi_{i,n} = \eta^2\left[1 + \left[\frac{E_{\theta,n}}{E_{r,n}}\right]^2\right]^{-1} \sim \frac{n^2}{k_1^2 r^2},$$

for either ψ- or ζ-waves and Q_n is the second solution of eq (60).

The Q-L approximation can be replaced by the full magneto-ionic theory by evaluating the index of refraction, η, from eqs (23 and 24) and employing the exact expression for P and Q in eqs (49, 50, 51, 52, 53) [Johler and Harper, 1962];

$$P_{me} = \frac{-\left[a_L\zeta + \frac{h_T h_L}{s(s^2-h^2)}\right]\left[1 - a_L^2 - \zeta^2 - \frac{s}{s^2-h^2}\right] + \left[a_L a_T - i\frac{h_L}{s^2-h^2}\right]\left[a_T\zeta - i\frac{h_T}{s^2-h^2}\right]}{\left[1 - a^2 - \frac{s^2-h_L^2}{s(s^2-h^2)}\right]\left[1 - a_L^2 - \zeta^2 - \frac{s}{s^2-h^2}\right] - \left[a_T\zeta + i\frac{h_T}{s^2-h^2}\right]\left[a_T\zeta - i\frac{h_T}{s^2-h^2}\right]},$$

$$-Q_{me} = \frac{-\left[1 - a^2 - \frac{s^2-h_L^2}{s(s^2-h^2)}\right]\left[a_L a_T - i\frac{h_L}{s^2-h^2}\right] + \left[a_T\zeta + i\frac{h_T}{s^2-h^2}\right]\left[a_L\zeta + \frac{h_L h_T}{s(s^2-h^2)}\right]}{\left[1 - a^2 - \frac{s^2-h_L^2}{s(s^2-h^2)}\right]\left[1 - a_L^2 - \zeta^2 - \frac{s}{s^2-h^2}\right] - \left[a_T\zeta + i\frac{h_T}{s^2-h^2}\right]\left[a_T\zeta - i\frac{h_T}{s^2-h^2}\right]},$$

The coefficients of the matrices in eqs 31 and 32 are:

$$a_{11} = a_{22} = a_{33} = \frac{m_e}{e^2 N_e}\left(-i\omega - \Sigma_1 + \frac{C_1 C_{12}}{\Sigma_1}\right)$$

$$a_{12} = -a_{21} = \frac{\mu_o H_{m,z}}{-e N_e}$$

$$a_{13} = -a_{31} = \frac{\mu_o H_{m,y}}{e N_e}$$

$$a_{23}=-a_{32}=\frac{\mu_0 H_{m,x}}{-eN_e}=0, \text{ if } \overline{H}_m \text{ is in the } yz\text{-plane}$$

$$a_{14}=a_{25}=a_{36}=\frac{m_e}{e^2N_+}\left(C_3+\frac{C_1C_{11}}{\Sigma_{10}}\right)$$

$$a_{17}=a_{28}=a_{39}=\frac{m_e}{e^2N_-}\left(C_2+\frac{C_1C_{10}}{\Sigma_{10}}\right)$$

$$a_{41}=a_{52}=a_{63}=\frac{m_+}{e^2N_e}\left(C_6-\frac{C_4C_{12}}{\Sigma_{10}}\right)$$

$$a_{44}=a_{55}=a_{66}=\frac{m_+}{e^2N_+}\left(-i\omega-\Sigma_4-\frac{C_4C_{11}}{\Sigma_{10}}\right)$$

$$a_{45}=-a_{54}=\frac{\mu_0 H_{m,z}}{eN_+}$$

$$a_{46}=-a_{64}=\frac{\mu_0 H_{m,y}}{-eN_+}$$

$$a_{56}=-a_{65}=\frac{\mu_0 H_{m,x}}{eN_+}=0, \text{ if } \overline{H}_m \text{ is in the } yz\text{-plane}$$

$$a_{47}=a_{58}=a_{69}=\frac{m_+}{e^2N_-}\left(C_5-\frac{C_4C_{10}}{\Sigma_{10}}\right)$$

$$a_{71}=a_{82}=a_{93}=\frac{m_-}{e^2N_e}\left(C_9\,\frac{C_7C_{12}}{\Sigma_{10}}\right)$$

$$a_{74}=a_{85}=a_{96}=\frac{m_-}{e^2N_+}\left(C_8+\frac{C_7C_{11}}{\Sigma_{10}}\right)$$

$$a_{77}=a_{88}=a_{99}=\frac{m_-}{e^2N_-}\left(-i\omega-\Sigma_7+\frac{C_7C_{10}}{\Sigma_{10}}\right)$$

$$a_{78}=-a_{87}=\frac{\mu_0 H_{m,z}}{-eN_-}$$

$$a_{79}=-a_{97}=\frac{\mu_0 H_{m,y}}{eN_-}$$

$$a_{89}=-a_{98}=\frac{\mu_0 H_{m,x}}{-eN_-}=0, \text{ if } \overline{H}_m \text{ is in the } yz \text{ plane}$$

where the C_i are defined in eq (29) and $\Sigma_i=C_i+C_{i+1}+C_{i+2}$.

$$b_{11}=a_L^2+\zeta^2-1$$

$$b_{12}=-a_L a_T$$

$$b_{13}=-a_T\zeta$$

$$b_{21}=-a_T a_L$$

$$b_{22}=\zeta^2+a_T{}^2-1$$

$$b_{23}=-a_L\zeta$$

$$b_{31}=a_L\zeta$$

$$b_{32}=a_L a_T$$

$$b_{33}=a_T{}^2+a_T a_L-1.$$

It is clear that a fundamental difficulty exists in treating anisotropic media with the wave eq (55). Thus, the separation of variables, eq (56), depends upon the assumption of isotropic media of propagation, i.e., k_3 must be independent of position and direction of propagation. Indeed, the complications introduced by such considerations have only been satisfactorily resolved in plane coordinates by treating Maxwell's equations directly. The procedure which has been outlined in this paper introduces such solutions of the magneto-ionic theory *ad hoc* to the rigorous series of zonal harmonics. This is a specification for the plasma medium k_3 which is an approximation. The validity of this approximation at long wavelengths depends on the behaviour of the complex index of refraction with respect to direction of propagation, such as the ratio, $E_{\theta,n}/E_{r,n}$, for elementary spherical wave, which can be readily computed with the aid of methods described in this paper. Also, the index of refraction, for $\sin\phi_i = \sin\phi_{i,n}$ dependence on ϕ and n can be evaluated. If $n \ll k_1 c$, $E_{\theta,n}/E_{r,n}$ for each wave type 1, 2 is almost real. Also, if $n \sim k_1 c$ an elliptical polarization can be noted, since $[E_{\theta,n}/E_{r,n}]_{1,2}$ are each complex. Furthermore, if $n \gg k_1 c$, each $[E_{\theta,n}/E_{r,n}]_{1,2}$ becomes imaginary indicating circular state of polarization.

The introduction of these complex numbers, $\sin\phi_i$, into the quartic eq (23) results in an approximately constant index of refraction, η for electron densities, $N=50-1000$ electrons/cm^2 over all distances, $d=a\theta$, for values of $n \sim 0$ to 10 $k_1 c$, $k_1 c \sim 10-1000$. This is especially true in the more important region $n \sim k_1 c$. This is consistant with the demonstrated validity of the $Q-L$ approximation at long wavelengths [Johler and Walters, 1960]. The degree to which the method of introducing the magneto-ionic theory to the rigorous series of zonal harmonics can be extrapolated to shorter wavelengths or higher frequencies is worthy of further investigation. Otherwise, it is necessary to return to Maxwell's eq (1) and reformulate the problem. It is anticipated, however, that the essential features of the magneto-ionic theory, such as the effect of the direction of the earth's magnetic field vector, the effect of polarization coupling external to the ionosphere, and the effect of the heavy ions can be adequately treated at long wavelengths with this theory.

(Paper 66D–234)